Distribution of Callose Synthase, Cellulose Synthase, and Sucrose Synthase in Tobacco Pollen Tube Is Controlled in Dissimilar Ways by Actin Filaments and Microtubules[1][W]

Giampiero Cai*, Claudia Faleri, Cecilia Del Casino, Anne Mie C. Emons, and Mauro Cresti

Dipartimento Scienze Ambientali "G. Sarfatti," Università di Siena, 53100 Siena, Italy (G.C., C.F., C.D.C., M.C.); Laboratory of Plant Cell Biology, Wageningen University, 6708 PB Wageningen, The Netherlands (A.M.C.E.); and Department of Biomolecular Systems, Foundation for Fundamental Research on Matter Institute for Atomic and Molecular Physics, 1098 SJ Amsterdam, The Netherlands (A.M.C.E.)

Callose and cellulose are fundamental components of the cell wall of pollen tubes and are probably synthesized by distinct enzymes, callose synthase and cellulose synthase, respectively. We examined the distribution of callose synthase and cellulose synthase in tobacco (*Nicotiana tabacum*) pollen tubes in relation to the dynamics of actin filaments, microtubules, and the endomembrane system using specific antibodies to highly conserved peptide sequences. The role of the cytoskeleton and membrane flow was investigated using specific inhibitors (latrunculin B, 2,3-butanedione monoxime, taxol, oryzalin, and brefeldin A). Both enzymes are associated with the plasma membrane, but cellulose synthase is present along the entire length of pollen tubes (with a higher concentration at the apex) while callose synthase is located in the apex and in distal regions. In longer pollen tubes, callose synthase accumulates consistently around callose plugs, indicating its involvement in plug synthesis. Actin filaments and endomembrane dynamics are critical for the distribution of callose synthase and cellulose synthase, showing that enzymes are transported through Golgi bodies and/or vesicles moving along actin filaments. Conversely, microtubules appear to be critical in the positioning of callose synthase in distal regions and around callose plugs. In contrast, cellulose synthases are only partially coaligned with cortical microtubules and unrelated to callose plugs. Callose synthase also comigrates with tubulin by Blue Native-polyacrylamide gel electrophoresis. Membrane sucrose synthase, which expectedly provides UDP-glucose to callose synthase and cellulose synthase, binds to actin filaments depending on sucrose concentration; its distribution is dependent on the actin cytoskeleton and the endomembrane system but not on microtubules.

The plant cell wall is composed of cellulose microfibrils (CMFs) embedded in the cell wall matrix, a mixture of polysaccharides, glycoproteins, and phenolic substances that interact with each other to generate an elaborate three-dimensional structure fundamental for plant cell development and plant stature. The construction of the cell wall in plant cells is a complex process that starts in the endoplasmic reticulum with the production of enzymes, which are subsequently processed in the Golgi bodies together with polysaccharides. Enzymes travel by membrane trafficking through the Golgi system and end up inside Golgi vesicles and their membrane, which is inserted into the plasma membrane, while the content of vesicles is secreted by exocytosis into the existing cell wall (Miller et al., 1997; Mutwil et al., 2008).

CMFs are crystalline, parallel β-1,4-glucan chains that are synthesized at the plasma membrane by the cellulose synthase complex (CSC), a multiprotein apparatus that presumably consists of 36 individual cellulose synthase (CesA) catalytic subunits (Persson et al., 2007; Guerriero et al., 2010). In the intercalary growing cells of the Arabidopsis (*Arabidopsis thaliana*) hypocotyl, CSCs have been observed to be inserted at sites of the plasma membrane where Golgi bodies are also positioned (Crowell et al., 2009; Gutierrez et al., 2009); furthermore, actin filament (AF)-depolymerizing drugs disrupt the distribution of CSCs (Gutierrez et al., 2009). At the level of individual delivery events, "small CesA-containing compartments" (Gutierrez et al., 2009) associate with cortical microtubules (MTs; Crowell et al., 2009; Gutierrez et al., 2009) and are preferentially delivered to sites where cortical MTs are present (Gutierrez et al., 2009). The regulation of CesA activity has also been suggested to involve the internalization of CSCs into membrane compartments associated with MTs (Crowell et al., 2009). During cell wall thickening in local secondary wall formation, Golgi bodies move along AFs and stop temporarily at sites where CSCs are to be delivered to the plasma membrane, but it is not known if Golgi vesicles move

[1] This work was supported by the Human Frontier Science Program (project no. RGP0018/2006–C), by the Research Program of Siena University and Ministry of University and Research 2008 (Research Projects of National Interest), and by the European Union Commission (grant no. FP6–2004–NEST–C1–028974 to A.M.C.E.).

* Corresponding author; e-mail cai@unisi.it.

The author responsible for distribution of materials integral to the findings presented in this article in accordance with the policy described in the Instructions for Authors (www.plantphysiol.org) is: Giampiero Cai (cai@unisi.it).

[W] The online version of this article contains Web-only data.
www.plantphysiol.org/cgi/doi/10.1104/pp.110.171371

along AFs in the final delivery step (Wightman and Turner, 2008, 2010). In addition, MTs also direct the movement of CSCs in the plasma membrane of intercalary elongating cells during the production of CMFs (Paredez et al., 2006; DeBolt et al., 2007a, 2007b; Desprez et al., 2007; Persson et al., 2007; Lloyd and Chan, 2008; Lucas and Shaw, 2008; Crowell et al., 2009; Gutierrez et al., 2009). However, the mode of interaction between MTs and the CSCs is not known.

In some plant cells, the cell wall matrix also contains callose, a β-1,3-linked Glc polymer with 1,6-branches (Chen and Kim 2009). The polymer is synthesized at many locations during plant development and in response to biotic/abiotic stress by callose synthase (CalS; Verma and Hong, 2001). Interaction of CalS with the cytoskeleton is largely unclear. In the liverwort *Riella helicophylla*, immunocytological analysis revealed that MTs do not occur at the sites of callose deposition (Scherp et al., 2002). However, in cells of Arabidopsis and tobacco (*Nicotiana tabacum*) treated with oryzalin, the enzyme activity of CalS is significantly reduced, suggesting that an intact MT cytoskeleton is required for proper callose synthesis (Aidemark et al., 2009). In BY-2 cells, the correct deposition of callose requires proper MT dynamics because inhibition of MT depolymerization reduced callose synthesis (Yasuhara, 2005). Interaction between AFs and CalS is not known; however, in the secondary vascular tissues of angiosperms and gymnosperms, myosin, AFs, and callose were observed around the pores of sieve elements and sieve cells (Chaffey and Barlow, 2002).

Production of cellulose and callose requires UDP-Glc (UDPG) that is likely to be provided by cleaving Suc molecules, a process carried out by Suc synthase (Sus). Sus is mainly restricted to tissues that metabolize Suc (Konishi et al., 2004) and is localized in different cell structures, such as close to the cytoskeleton, the tonoplast, and other membranes (Matic et al., 2004). While a soluble form of Sus is generally involved in the cytoplasmic metabolism of Suc, a membrane form of Sus is associated with the plasma membrane or cell wall and has been suggested to provide UDPG for CalS and CesA (Amor et al., 1995). A direct association between Sus and CesA is a debated question. Although some authors suggest that there is no evidence for direct interactions between CesA and Sus (Guerriero et al., 2010), cooperation between Sus and CesA is supported by many indirect findings. For example, Sus is associated with thickenings of the secondary cell wall in cotton (*Gossypium hirsutum*) fibers (Salnikov et al., 2003), and two Sus isoenzymes of maize (*Zea mays*) have a critical role in the synthesis of cellulose (Chourey et al., 1998). In roots of wheat (*Triticum aestivum*) under hypoxic conditions, the increased enzyme activity of Sus overlapped the deposition pattern of cellulose (Albrecht and Mustroph, 2003). Recently, the catalytic unit of CesA was found to be enriched with a polypeptide identified as Sus by mass spectrometry and immunoblotting (Fujii et al., 2010). An association of Sus with CalS has not yet been demonstrated, but some reports indicate that CalS may be associated (directly or indirectly) with Sus (Amor et al., 1995; Hong et al., 2001). The evidence that pollen tubes have an internal concentration of UDPG above the K_m of CalS (Schlupmann et al., 1994) suggests that a membrane-associated Sus is not required to deliver the substrate directly to the plasma membrane-associated CalS. Nevertheless, Sus may be required for the maintenance of local higher concentrations of UDPG in order to fuel the molecular mechanism that delivers UDPG to CalS. Some authors (Guerriero et al., 2010) propose that UDPG may be synthesized by two different mechanisms (one based on UDPG pyrophosphorylase, the other based on Sus), but no critical proofs are available to validate one or the other. The evidence that Sus is an actin-binding protein led to the proposal that Sus associates with CalS or CesA at the plasma membrane, thus establishing a spatial context for the work of a multiprotein complex that facilitates cellulose and callose synthesis (Salnikov et al., 2001).

The pollen tube is a cell extension that the pollen grain produces upon germination on a receptive stigma, and its main function is to carry sperm cells to the embryo sac (Higashiyama et al., 2003). The pollen tube elongates by tip growth, a mechanism of cell expansion confined to the apex, where many secretory vesicles fuse with the plasma membrane (Parton et al., 2001; Ketelaar et al., 2008). Accumulation of Golgi-derived secretory vesicles in the tube tip is supported by a polarized actin cytoskeleton, which drives and focuses vesicles into the growth region (Geitmann and Emons, 2000; for review, see Cole and Fowler, 2006). Golgi vesicles, which supposedly contain CesA and CalS in their membranes, are present in the cell tip, probably not attached to Golgi bodies (Ketelaar et al., 2008); vesicles are continuously delivered from the basal part of the cell and consumed at the tip during cell growth. Although vesicle transport could occur by diffusion, the focusing activity of the actin fringe at the border of the vesicular area in pollen tubes (Lovy-Wheeler et al., 2005) and the subapical fine F-actin configuration in root hairs (Miller et al., 1999; Ketelaar et al., 2003) play roles in vesicle positioning. In pollen tubes, AFs polarize the cytoplasm at the tube apex (Vidali and Hepler, 2001; Vidali et al., 2001; Lenartowska and Michalska, 2008) and regulate the reversal of organelle movement (Cárdenas et al., 2005) by progressively extending the cortical actin fringe. The fringe could also be used as a track to deliver secretory vesicles to exocytotic sites (Bove et al., 2008; Cárdenas et al., 2008). On the other hand, the role of MTs in pollen tube growth is still unclear, even though MTs have been shown to be involved in organelle/vesicle transport/localization in vitro (Cai and Cresti, 2009, 2010).

Anisotropic pollen tube development and polarization of membranes and cytoskeleton are also reflected in the nonuniform distribution of the cell wall com-

ponents. The apical region of pollen tubes is characterized by a pectin layer (Li et al., 1995) that extends for the entire tube length and forms the outer cell wall layer. This pectin layer is progressively substituted by a secondary inner layer, mainly consisting of callose (around 81%) and cellulose (only 10%; Schlupmann et al., 1994). Although with the use of specific probes, cellulose and callose were not detected in the tube tip (Ferguson et al., 1998), electron microscopy after freeze fracturing has shown cellulose microfibrils in a direct way in this location (Kroh and Knuiman, 1982). Callose is present from 30 μm behind the tip (Ferguson et al., 1998) and in callose plugs (Cresti and van Went, 1976; Ferguson et al., 1998). Callose is produced by CalS, a protein localized in the plasma membrane (Ferguson et al., 1998), and activated in vitro by proteolysis and detergents (Brownfield et al., 2007). CalS in *Nicotiana alata* pollen tubes consists of a 220-kD polypeptide, which is likely to be delivered to the plasma membrane by exocytosis of Golgi membranes (Brownfield et al., 2008). The gene coding for the pollen tube CalS has not yet been identified, but the *N. alata* glucan synthase-like 1 (NaGSL1) gene has been proposed to encode the CalS of *N. alata* pollen tubes on the basis of several findings. The gene sequence is highly similar to the fungal 1,3-β-glucan synthase and is highly expressed in pollen tubes; partially purified CalS contained a 220-kD polypeptide corresponding to the predicted molecular mass of NaGSL1; the protein was detected by an anti-glucan synthase antibody and was identified as NaGSL1 using matrix-assisted laser-desorption ionization time of flight mass spectrometry and liquid chromatography-ESI-tandem mass spectrometry analysis of peptides (Brownfield et al., 2007). The above evidence indicates that NaGSL1 is a strong candidate for CalS. Cellulose occurs in lower quantities than callose (Schlupmann et al., 1994). Since it is a crystalline component, the orientation of cellulose is potentially important for the architecture of the cell wall (Ferguson et al., 1998) and for pollen tube growth (Anderson et al., 2002). Furthermore, mutation in a CesA-like sequence of Arabidopsis indicated that the gene product is important for pollen tube growth (Goubet et al., 2003). In the pollen tube, Sus is distributed at both the plasma membrane and the cell wall, with higher levels detected in the apical and subapical regions. The enzyme activity of Sus is mainly directed to Suc cleavage, and the enzyme exists at least as two isoforms that are differently distributed among cell compartments. The availability of Suc in the germination medium affects the content and intracellular distribution of Sus (Persia et al., 2008), with Sus mostly detected in the plasma membrane and cell wall fractions during active growth but found in the cytoplasm during slower growth. This suggests that Suc is a general regulator of Sus activity in the pollen tube.

The pollen tube is an excellent cell type to study the contribution of AFs, MTs, and membrane dynamics in establishing the correct cellular distribution of CalS, CesA, and Sus. Pollen tubes produce both callose and cellulose at specific locations and at specific moments during growth. They possess distinct arrays of MTs and AFs, which are related to pollen tube growth and along which organelles, including Golgi bodies, move. We show that CesA and CalS distribute differently in the plasma membrane of tobacco pollen tubes. While CesA is present mostly in the apical domain and to a lesser extent in the remaining cortical region, CalS is present in the apical domain, in distal regions, and in regions where callose plugs are being formed, consistent with its role in the deposition of these plugs. The overall distribution of apical CalS, CesA, and Sus is controlled by AFs, while the distribution of distal CalS is primarily controlled by MTs, with which they associate in Blue Native-PAGE experiments. Membrane Sus binds to AFs and comigrates with actin in Blue Native-PAGE experiments.

RESULTS

Antibodies Prepared to CalS Are Specific and Do Not Cross-React with Other Proteins

We raised two antisera against conserved peptides in the amino acid sequence of CalS from Arabidopsis and *N. alata*. The antibody DDA was raised against a peptide sequence located at the C-terminal domain of CalS and belonging to the glucan synthase domain (Fig. 1A). The antibody HDA was raised against two peptides at the N terminus of both *Nicotiana* and Arabidopsis CalS that do not belong to the domain of glucan synthase. As expected, the antiserum efficiently cross-reacted with different quantities of antigenic peptides conjugated to keyhole limpet hemocyanin (KLH; Fig. 1B). As a further control, the secondary antibody alone did not cross-react with the antigenic peptide (lane Ag+2Ab). Subsequently, HDA was assayed by immunoblot on cytosolic proteins (Fig. 1C, lane 2), membrane proteins (lane 3), and cell wall proteins (lane 4) from tobacco pollen tubes; extract of mature Arabidopsis flowers (lane 5) was also assayed. The antibody cross-reacted with a polypeptide of 225 kD in the protein pool from membrane and cell wall fractions of pollen tubes as well as in Arabidopsis extracts. To validate these results, HDA was affinity purified by absorption of nitrocellulose membranes coated with peptide antigens (Fig. 1D); the final sample contained the presumptive heavy and light chains of HDA antibody (lane 4, arrow and arrowhead). The antigen unbound antibody fraction (lane 3 of Fig. 1D) did not cross-react with cytosolic proteins (Fig. 1E, top panel, lane 1), membrane proteins (lane 2), and cell wall proteins (lane 3) from pollen tubes and against Arabidopsis extracts (lane 4). On the contrary, the bound/released antibody fraction (lane 4 of Fig. 1D) efficiently cross-reacted with all samples except for cytoplasmic proteins (Fig. 1E, bottom panel). The molecular mass and the distribution pattern of the polypeptide recognized by DDA antibody were virtually comparable to those recognized by HDA (for the

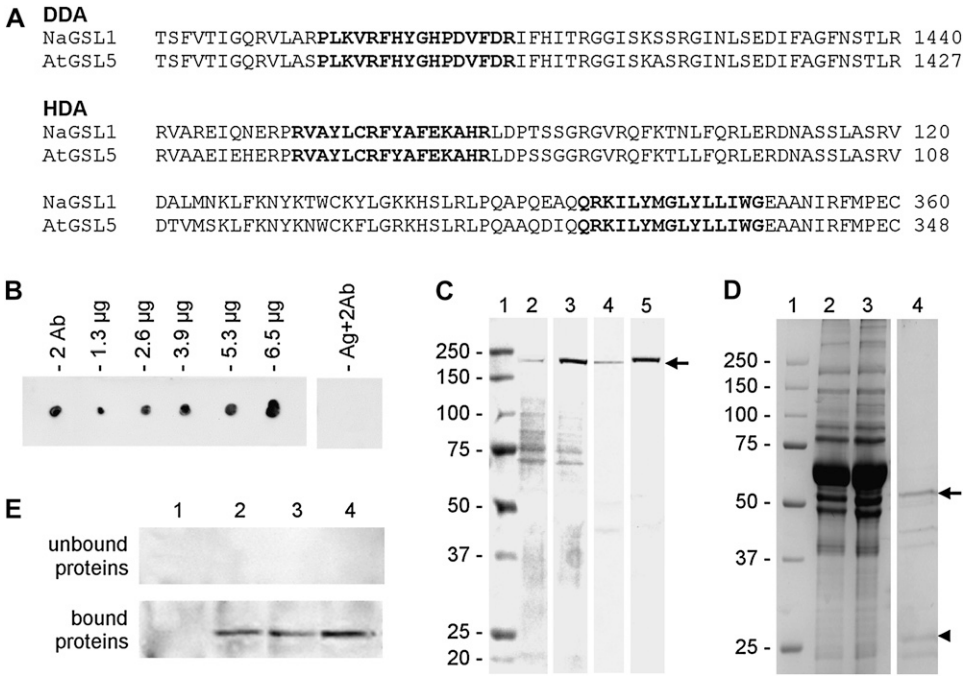

Figure 1. Characterization of antibodies to CalS. A, Sequences of CalS used for the production of peptide antibodies. The antibody DDA was raised against a peptide sequence (in boldface) located at the C-terminal domain of CalS. The antibody HDA was raised against two peptide sequences (in boldface) found at the N-terminal domain of both *N. alata* (Na) and Arabidopsis (At) CalS. In both cases, numbers on the right indicate the positions of sequences in the protein. B, Dot blot showing the characterization of HDA; the antibody was assayed without antigen (2 Ab) on 1.3, 2.6, 3.9, 5.3, and 6.6 μg of antigen peptides conjugated to KLH; as a control, the antigen peptide was also tested with the secondary antibody only (Ag+2Ab). C, Immunoblot showing the screening of HDA antibody on cytosolic proteins from tobacco pollen tubes (lane 2), membrane proteins (lane 3), and cell wall proteins (lane 4) from tobacco pollen tubes in addition to extract from Arabidopsis flowers (lane 5); a polypeptide of 225 kD is prominently recognized in lanes 3 to 5. About 30 μg of protein was loaded in each lane. Prestained M_r markers were loaded in lane 1. All lanes are from the same blot. D, SDS-PAGE showing the partial purification of HDA antibody by absorption of nitrocellulose membranes coated with antigen peptides. Lane 1, Markers of M_r; lane 2, starting antiserum; lane 3, unbound proteins; lane 4, absorbed proteins released by acid solution (purified antibody). Arrow and arrowhead indicate the presumptive heavy and light chains of HDA antibody, respectively. E, Cross-reactivity of antigen-unbound proteins (sample in lane 3 of D) and of antigen-bound proteins (the purified antibody, lane 4 of D) against cytosolic proteins (lane 1), membrane proteins (lane 2), and cell wall proteins (lane 3) from pollen tubes and against extracts of Arabidopsis flowers (lane 4). Lanes contain 30 μg of proteins.

characterization of DDA, see Supplemental Fig. S1), suggesting that the peptide sequences used as antigen belong to the same or related polypeptide chains.

CalS Localizes Both to the Apical Domain and to Distal Regions of Pollen Tubes

The HDA antibody was used to determine the intracellular distribution of CalS using immunofluorescence microscopy. In short pollen tubes after 30 min of growth (around 40 μm), CalS was mainly detected in the apical domain as a cap in the first 10 μm (Fig. 2A, arrow). This region approximately corresponds to the growth area where secretory vesicles and endocytotic vesicles are observed with the electron microscope. This domain was followed by a less intense labeling area, which covered the remaining tube length (Fig. 2A, arrowhead). When observed at focal planes tangential to the tube cortex, the apical region of pollen tubes showed a punctate pattern of labeling (Fig. 2B1); higher magnification images at the apex/subapex interface showed several spots below the plasma membrane reminiscent of the distribution of vesicles (Fig. 2B2). In longer pollen tubes after 70 min of growth (about 80 μm in length), staining was again prominent in the apical domain and in the tube restricted to the cortex. In addition, a high density of CalS was observed in distal segments of the pollen tube (Fig. 2C, arrow). In longer tubes after 90 min of growth (more than 100 μm), labeling was present in three distinct regions (Fig. 2D): a strong apical staining (arrow), an intermediate region characterized by slighter staining (arrowhead), and a distal segment in which labeling was stronger again (bordered arrow). The length of segments occupied by each location was quantified in 3-h-grown pollen tubes by measuring the fluorescence intensity along the shank of pollen tubes, from the tip down to the base region (Fig. 2E). Values

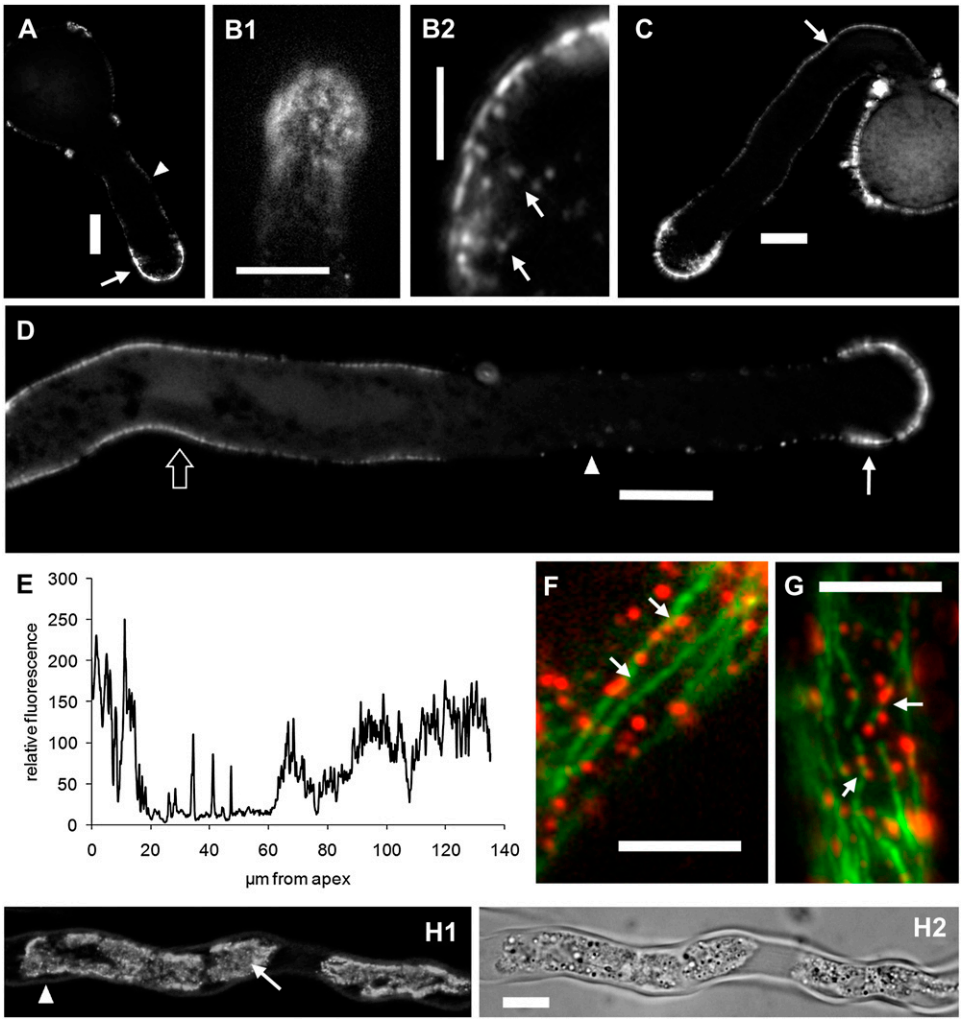

Figure 2. Distribution of CalS as shown by HDA antibody in immunofluorescence microscopy. Images in A, C, and D are single focal planes obtained in the tube center, while images in B and F are focused at the tube cortex. A, In short pollen tubes, labeling of CalS was mainly found in the cortical region of the apical domain (arrow); labeling extended approximately for the first 20 μm. This region was followed by less intense labeling, which was located in the cortex of pollen tubes and extended toward the pollen grain (arrowhead). B, Magnification of the apical region of pollen tubes showing the dotted distribution pattern of CalS. B1, Image of a single focal plane tangential at the tube surface. B2, Magnification of a focal plane in the tube center highlighting the presence of fluorescent spots in proximity of the tube apex (arrows). C, In longer pollen tubes, the slightly fluorescent region was followed by a distal region in which fluorescence intensity increased (arrow). D, In even longer tubes, the three-patterned distribution of CalS is more evident: the apical stronger region (arrow), the intermediate slighter region (arrowhead), and the distal intense region (bordered arrow); in all cases, staining is mainly cortical. E, Measurement of fluorescence intensity along the shank of pollen tubes, from the tip down to the base region. The three-segmented distribution of CalS is evident. F and G, In double labeling experiments performed on untreated pollen tubes, CalS (red, arrows) was sometimes found to colocalize with microtubules (green). Bars = 10 μm (A, B1, C, and D), 3 μm (B2), and 5 μm (F and G). H, Distribution of CalS in pollen tubes after plasmolysis. H1, Most of the CalS signal is found in the collapsing cytoplasm (arrow), and only a faint signal is found in the cell wall (arrowhead). H2, Corresponding DIC image. Bar = 10 μm.

are averages of data collected on different pollen tubes (at least 20 pollen tubes) with equivalent length. The fluorescence profile shows that CalS is distinctly distributed in the initial 15 to 20 μm of the pollen tube and, after a lower intensity segment of 40 to 60 μm, it reappears at higher abundance around 100 μm from the tube tip. Autofluorescence in control pollen tubes (without primary antibody) was practically absent and therefore is not included in the graph. When pollen tubes were stained for CalS and tubulin, we often found colocalization of CalS spots (red) with MTs (green) in distal regions, corresponding to the third segment of labeling where the presence of CalS is more abundant (Fig. 2, F and G, arrows). To quantify the colocalization between CalS and MTs, we analyzed several double immunofluorescence images (n = 10;

single focal planes) for the following correlation coefficients using the JACoP plugin for ImageJ (http://rsb.info.nih.gov/ij/plugins/track/jacop.html). The Pearson correlation coefficient was 0.63; the Manders (overlap) coefficient was 0.84 with M1 (fraction of CalS overlapping MTs) corresponding to 0.81 and M2 (fraction of MTs overlapping CalS) equivalent to 0.24; the Van Steensel cross-correlation coefficient showed a bell-shaped curve peaking to one side. All these coefficients indicate a consistent (although not complete) colocalization between CalS dots and cortical MTs. Association of CalS with the plasma membrane of pollen tubes was also shown by plasmolysis (Fig. 2, H1 and H2); after plasmolysis, most of the CalS signal was retained in the collapsing cytoplasm (arrow), while a faint signal remained in the cell wall (arrowhead).

In longer pollen tubes (more than 9 h of growth, around 900 μm long), four to five callose plugs had been formed, with the first callose plug forming after 4 h of growth, around 300 μm of pollen tube length (for statistical evaluation of callose plug formation, see Laitiainen et al., 2002). We found that CalS accumulated during the development of callose plugs, which were easily observable using differential interference contrast (DIC) microscopy (Fig. 3A, arrow). When the same plug was observed after anti-CalS labeling (Fig. 3B), we noted a considerable increase of CalS on both sides of the callose plug; labeling was lost in the older mature (central) region of the plug (asterisk). On the side of the developing plug, CalS was distributed as dots, apparently aligned along the border of the callose plug (Fig. 3B, arrows). In most of the pollen tubes, the region around plugs (Fig. 3C, arrow) was strongly labeled by anti-CalS, revealing a consistent accumulation of CalS around the callose plug (Fig. 3D, in red). In the same samples, MTs were observed to pass through the plug hole longitudinally, mixed with several CalS dots (Fig. 3D, in green). Colocalization of CalS and MTs around the callose plug is suggested at higher magnification in double labeling experiments. CalS dots (Fig. 3E, in red, arrows) appeared as aligned along cortical MTs (in green) on the side of the growing plug. The Pearson coefficient was 0.70, while the Manders coefficients were M1 = 0.71 (fraction of CalS overlapping MTs) and M2 = 0.29 (fraction of MTs overlapping CalS); in addition, the Van Steensel cross-correlation coefficient again showed a bell-shaped curve peaking on one side. We also analyzed the distribution of Sus in and around the

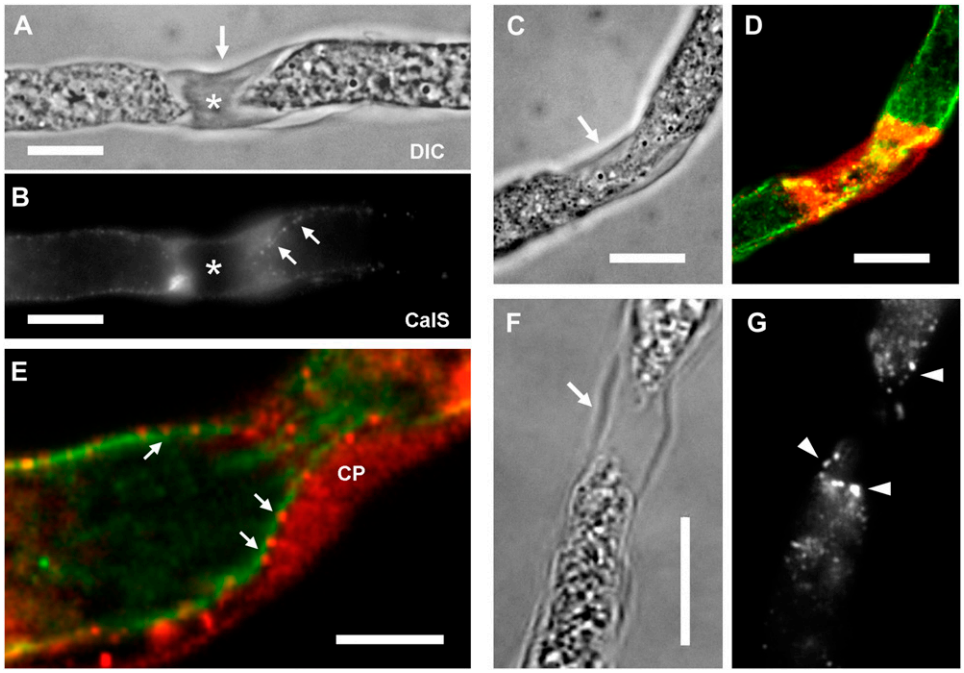

Figure 3. Localization of CalS in the callose plugs of pollen tubes. Longer pollen tubes (about 9 h of growth) were labeled by anti-CalS in order to analyze the distribution of CalS in comparison with callose plugs. A, A developing callose plug, which was observable using DIC microscopy (arrow). B, The same plug observed after immunostaining with anti-CalS showed a substantial increase of CalS on both sides, but labeling was absent on the central mature region of the plug (asterisk). On the side of the growing plug, CalS appeared as dots aligned along the border of the callose plug (arrows). Bars = 10 μm. C and D, One pollen tube with a developing callose plug (C, arrow) also showed a strong labeling by anti-CalS antibody around the plug (D; in red); MTs appeared as strands still passing through the narrow hole formed by the plug (D; in green). Bars = 10 μm. E, At higher magnification, CalS (in red) appeared as dots (arrows) aligned on cortical MTs (in green) on the side of the growing callose plug (CP). Bar = 5 μm. F and G, Analysis of Sus distribution at the level of callose plugs. When a callose plug formed (indicated by the arrow in the DIC image in F), the relative amount of Sus in its proximity increased significantly and prominent accumulation of Sus on both sides of the callose plugs was observed (G; arrowheads). Bar = 20 μm.

callose plugs. Most of the membrane Sus in tobacco pollen tubes was associated with the cortical region (plasma membrane and cell wall), with a considerably higher concentration in the proximity of callose plugs (arrow in the DIC image in Fig. 3F). We regularly observed an accumulation of Sus on both sides of the callose plugs (Fig. 3G, arrowheads).

Quantitative information on the distribution of CalS in pollen tubes was obtained by immunogold electron microscopy. We analyzed different regions of tobacco pollen tubes, the positions of which are approximately indicated by the drawing on the right side of Figure 4. The apical region of pollen tubes (Fig. 4A) was characterized by a large number of gold particles (563 ± 47 gold particles μm^{-2}), which were mostly concentrated at the interface between the plasma membrane and the cell wall. A limited number of gold particles were also found in the pollen tube cytoplasm (25 ± 11 gold particles μm^{-2}), whereas very few (most likely nonspecific) particles were found outside of the pollen tube. When particles were counted using the ImageJ software, the cell wall region (probably comprising the plasma membrane) accounted for more than 80% ± 5% of gold particles in each electron micrograph, while the pollen tube cytoplasm contained 20% ± 3% and the outside of pollen tubes (i.e. the inclusion resin) accounted for only 1% ± 0.5% of particles. Images at the level of the subapex showed gold particles in close association with vesicle-like structures (Fig. 4B), suggesting that CalS is transported to the plasma membrane inside the membrane of vesicles. The putative association of gold particles with the plasma membrane is more evident in magnified images (Fig. 4C, arrows). In the region next to the subapex, only a few gold particles could be detected (57 ± 13 gold particles μm^{-2}), in accordance with results of immunofluorescence microscopy. In such cases, the percentage of gold particles in the cell wall region matched that found in the cytoplasm (Fig. 4D). In more distal regions, the number of gold particles increased considerably (496 ± 41 gold particles μm^{-2}), and they still maintained their association with the plasma membrane and cell wall (Fig. 4E). This is the region where the first callose plug is expected to be formed (Cheung, 1996; Laitiainen et al., 2002). Again, gold particles in the cell wall region accounted for more than 85% ± 5% of total particles. When observed at higher magnification, gold particles in the distal region were found to line up consistently at the interface between cytoplasm and cell wall, presumably the plasma membrane (Fig. 4F, arrows). If the cell wall surface was arbitrarily divided into three consecutive regions (one closer to the plasma membrane, one intermediate, and the last in touch with the inclusion resin), more than 90% of gold

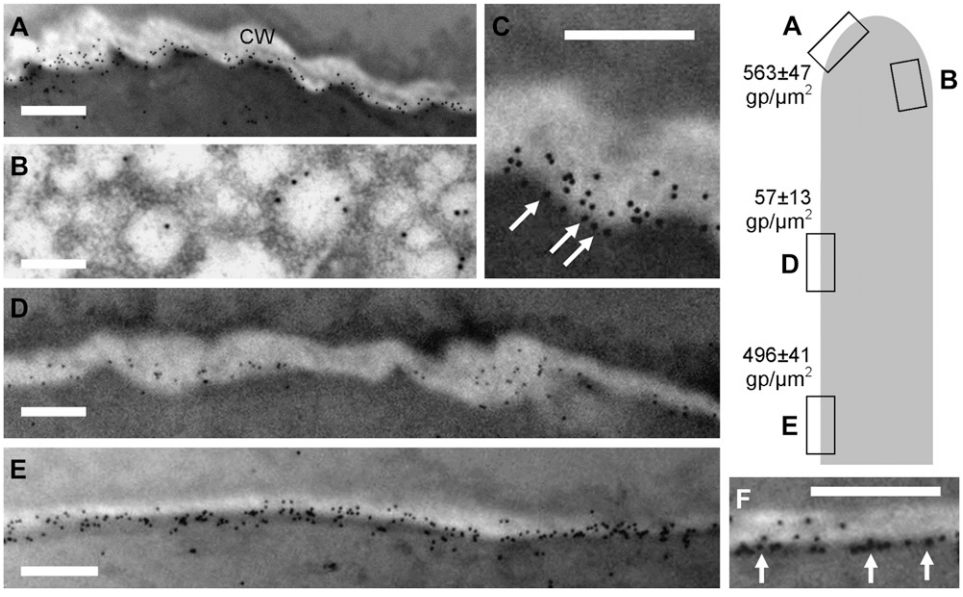

Figure 4. Immunogold electron microscopy of CalS in pollen tubes. The drawing on the right indicates the approximate position of the electron micrographs and the density of gold particles (gp) μm^{-2} in each sample. A, View of the apical region of pollen tubes. A large number of gold particles can be observed; most of them are concentrated at the plasma membrane/cell wall (CW) interface. Bar = 350 nm. B, Labeling of CalS in the apical region, suggesting an association with vesicle-like structures. Bar = 150 nm. C, Magnification of labeling in the apical domain showing the presumptive association of gold particles with the plasma membrane (arrows). Bar = 250 nm. D, View of CalS distribution in the intermediate region. Few gold particles can be detected. Bar = 350 nm. E, View of distal regions of pollen tubes. The number of gold particles at the plasma membrane/cell wall interface increased considerably. Bar = 350 nm. F, When observed at higher magnification, gold particles in the distal region were lined up at the plasma membrane/cell wall interface (arrows), suggesting an association with the plasma membrane. Bar = 250 nm.

particles were found in the first cell wall segment. We think that the electron micrographs showed undoubtedly the membrane localization of CalS; because of its size, the label of the antibody sticks out from the antigenic size at the electron microscopy resolution and could be responsible for the labeling in the pollen tube cell wall.

Distance between the different regions of Figure 4 was difficult to calculate, because pollen tubes were first embedded in a resin block, which was cut into smaller pieces before finely cutting on a ultramicrotome. On the basis of the "precut" (necessary to select specific regions), we can only affirm that Figure 4D is about 40 to 50 μm and that Figure 4E is around 90 to 100 μm from the pollen tube apex.

CesA Is Present All through the Pollen Tube Cortex

In order to monitor the distribution of CesA, we took advantage of an antiserum (generously provided by Prof. Chris Somerville) that cross-reacted with a conserved peptide sequence present in all CesA molecules (Gillmor et al., 2002). When tested on different protein extracts, the antiserum cross-reacted with a 125-kD polypeptide in the Arabidopsis extracts (Fig. 5A, lane 1), in the membrane protein fraction (lane 3), in the Triton-extracted cell wall proteins (lane 4), and weakly in the NaCl-extracted cell wall proteins (lane 5) from tobacco pollen tubes. The cross-reacting polypeptide was detected neither in the cytoplasmic protein pool (lane 2) nor in the SDS-solubilized protein fraction from the cell wall (lane 6). Background noise was noticeable in all lanes, but reaction was specific. We have not purified CesA; therefore, we did not test the reactivity of the anti-CalS antibody on purified CesA. In immunoblots, the anti-CesA and anti-CalS antibodies cross-reacted with proteins of different molecular mass (125 kD for CesA versus 225 kD for CalS). Although the immunolocalization pattern of the two proteins was occasionally similar in the pollen tube, the inhibitory experiments (see below) suggest that the two antigens belong definitely to different proteins. In addition, when the anti-CalS antibody was preabsorbed on the antigenic peptide, no signal was observed in immunoblots at the level of the CesA molecular mass. Evidence of CesA in the NaCl cell wall fraction raised the question of whether CesA in the cell wall is a contamination in the procedure. We think that the presence of CesA in the pollen tube cell wall is dependent on the extraction procedure, which probably leaves some plasma membrane remnants in association with the cell wall; in confirmation of this hypothesis, CesA could be easily removed by NaCl treatment.

The distribution of CesA proteins was different compared with CalS. When used in immunofluorescence microscopy, the CesA antiserum depicted a punctate pattern at the cell border, which was more evident in the apical domain (Fig. 5B, arrow) and progressively weaker in the remaining part of pollen tubes (arrowhead). Focal sections fixed at the tube center revealed that staining was found in the cortical region of pollen tubes, with the exception of the apical domain, where labeling was also detected in the cytoplasm (asterisk), probably in association with Golgi-derived vesicles. When the relative fluorescence intensity of CesA was measured along the tube border, the resulting graph confirmed a higher intensity of staining in the apical domain and a progressive decrease to constant levels at 40 to 50 μm from the tube apex (Fig. 5C). Compared with CalS staining, no additional labeled areas were found in distal segments of pollen tubes. The dotted nature of labeling was revealed by the high number of graph peaks and by distinct fluorescence dots observed in tangential focal planes (Fig. 5D). Measurement of the distance between spots in tangential focal planes (such as the one shown in Fig. 5D2) returned an average distance between adjacent spots of 0.78 ± 0.22 μm ($n = 100$). The density of fluorescent spots was 1.53 ± 0.14 per μm^2 ($n = 50$). In tangential focal planes at the level of the plasma membrane/cell wall (Fig. 5D1), CesA particles were abundantly present; sometimes, they aligned along invisible tracks (arrow), which might represent underlying MTs. In the same sample, with the focal plane just below the plasma membrane (0.3 μm from the previous one; Fig. 5D2), in the area where vesicles are present, CesA was localized in that region also in particles but with different alignment compared with the previous focal plane. At focal planes in the middle of the same pollen tube (Fig. 5D3), CesA was found only in the cortex. We also tested by double immunofluorescence microscopy the putative coalignment of CesA particles with MTs in the cortex of pollen tubes (Fig. 5, E and F). Although some CesA particles (red) occasionally aligned with MTs (green), we never found a precise codistribution between MTs and CesA proteins. The Pearson coefficient was only 0.32, while the Manders coefficients were M1 = 0.18 (fraction of CesA overlapping MTs) and M2 = 0.264 (fraction of MTs overlapping CesA); furthermore, the Van Steensel cross-correlation coefficient returned a three-peaked curve with only one peaking in the center. CesA particles were dispersed among MTs as well as positioned along MT bundles, suggesting that their relationship (if present) does not consist of precise coalignment. However, an in vivo study is required to make definitive statements here.

The distribution of CesA in the apical and subapical regions of pollen tubes was also investigated by immunogold labeling. CesA was mainly observed in association with the cortical region of tobacco pollen tubes, presumably with the plasma membrane (Fig. 5G, arrows). Gold particles were also found in association with vesicular structures just below the plasma membrane (Fig. 5G, arrowheads) and with Golgi bodies (bordered arrow). In general, the association of gold particles with the plasma membrane (Fig. 5H, arrow) and with vesicular structures of approximately 100 to 150 nm close to the plasma membrane (Fig. 5, I and J, asterisks) was the most prominent feature of CesA distribution.

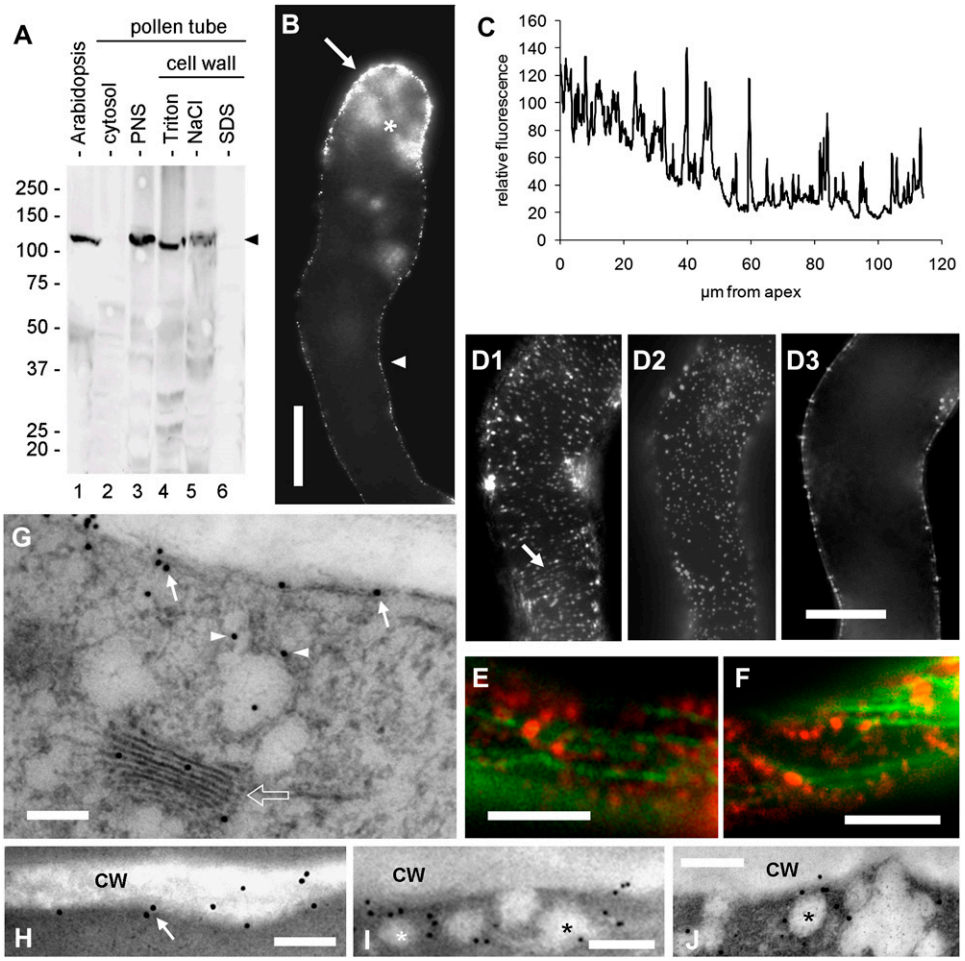

Figure 5. Characterization of CesA in tobacco pollen tubes. A, Immunoblot with anti-CesA antibody on Arabidopsis extract (20 μg; lane 1), cytosolic proteins (20 μg; lane 2), membrane proteins (20 μg; lane 3), Triton-solubilized cell wall proteins (10 μg; lane 4), NaCl-solubilized cell wall proteins (10 μg; lane 5), and SDS-solubilized cell wall proteins (5 μg; lane 6) from tobacco pollen tubes. The arrowhead indicates the main cross-reacting band around 125 kD in the Arabidopsis, membrane, Triton-, and NaCl-extracted proteins. B, Immunolocalization of CesA in tobacco pollen tubes. The image was captured in the center of the pollen tube. Staining was mainly observed in the apical domain (arrow) and to a lesser extent in the remaining cortical region (arrowhead). In the apex, staining was also diffusely observed in the cytoplasmic domain (asterisk), presumably in association with vesicular material. C, Measure of fluorescence intensity along the cell border of pollen tubes emphasizing the higher signal in the apex and the progressive decline toward a basal level. The presence of numerous peaks indicates the spot-like distribution of CesA proteins. D, A single pollen tube observed at three different focal planes: D1, tangential to the surface (presumably plasma membrane and cell wall); D2, just below the plasma membrane; D3, in the middle. CesA was distributed differently. The arrow indicates invisible tracks along which CesA spots align. Bar = 10 μm. E and F, Double immunolocalization of microtubules (green) and CesA (red). CesA proteins appeared as dots sometimes coaligning with microtubules but also distributed between microtubule bundles. Bars = 5 μm. G, Immunogold labeling of CesA. The protein was detected in association with the plasma membrane (arrows), with vesicular structures below the plasmalemma (arrowheads) and with Golgi bodies (bordered arrow). Bar = 250 nm. H to J, Immunogold labeling of CesA in the cortex of pollen tubes. CesA was mainly found in association with the cortical region of tobacco pollen tubes, presumably with the plasma membrane (H; arrow). Gold particles were frequently found in association with vesicular structures (asterisks) of around 100 to 150 nm that accumulate in proximity of the plasma membrane (I and J). Bars = 250 nm.

Biochemical Fractionation of Pollen Tube Membranes Shows that CalS, CesA, and Sus Are Associated with the Plasma Membrane

Immunofluorescence and electron micrographs show that CesA and CalS are associated with the cortical region of pollen tubes, expectedly with the plasma membrane. In order to determine the subcellular membrane compartment associated with CesA and CalS, we separated the membrane pool of 9- to 12-h-grown pollen tubes into 20 fractions by centrifugation along 8% to 65% continuous Suc gradients. In the SDS-PAGE of Figure 6A, only 17 out of 20 fractions are

shown, with fraction 1 corresponding to 8% and fraction 17 corresponding to 57% Suc. Fractions were assayed by immunoblot with anti-CesA antibody, which revealed the 125-kD band mainly in fractions 8 to 13 (Fig. 6B). CalS, visualized by immunoblot with HDA (Fig. 6C), and Sus, which was labeled by K2 antibody (Heinlein and Starlinger, 1989; Fig. 6D), sedimented approximately in the same fractions. A minor secondary peak of Sus was also found in fractions 4 and 5. As a control, the positions of both tubulin and actin were also tested using specific antibodies. Tubulin was found to distribute as a broader peak with a maximum in fraction 10, thus comparably to CesA, CalS, and Sus; on the other hand, actin distributed in all fractions, indicating that actin associates with a variety of intracellular membranes. Further confirmation of codistribution among CesA, CalS, and Sus was obtained by measuring their immunoblot profiles from three independent immunoblots and averaging their values; results show that CalS, CesA, and Sus peak around fraction 10 (Supplemental Fig. S2). When enzyme markers for different membrane compartments were analyzed, fraction 10 was found to be enriched in the plasma membrane marker P-ATPase, with other organelle markers sedimenting in different fractions (bottom part of Fig. 6).

Binding of Membrane Sus to Actin Filaments Requires Suc

Since Sus has been suggested to be an actin-binding protein (Winter et al., 1998), we analyzed the binding affinity between pollen Sus and AFs and its dependence on Suc concentration. At first, cytoplasmic Sus of pollen tubes was assayed for its affinity to AFs (Fig. 7A). After mixing cytosolic proteins of pollen tubes (lane 2) with AFs (lane 3) in the absence (lanes 8 and 9) and in the presence of either 40 mM Suc (lanes 10 and 11) or 100 mM Suc (lanes 12 and 13), the distribution of Sus was analyzed by immunoblot with anti-Sus antibody (Fig. 7B). As a result, cytoplasmic Sus bound to AFs in the absence of Suc (pellet of lane 9) but not in the presence of either 40 or 100 mM Suc (pellets of lane 11 and 13). When AFs were omitted, cytosolic proteins (Fig. 7A, lane 6) and Sus (Fig. 7B, lane 6) were found in the supernatant. In control samples, bovine serum albumin (BSA) was assayed for its binding capacity to AFs in either the absence of Suc (Fig. 7A, lanes 12 and 13) or in the presence of 40 and 100 mM Suc; in all cases, BSA was consistently found in the supernatant. Actin filaments alone were almost exclusively detected in the pellet (Fig. 7A, lane 5).

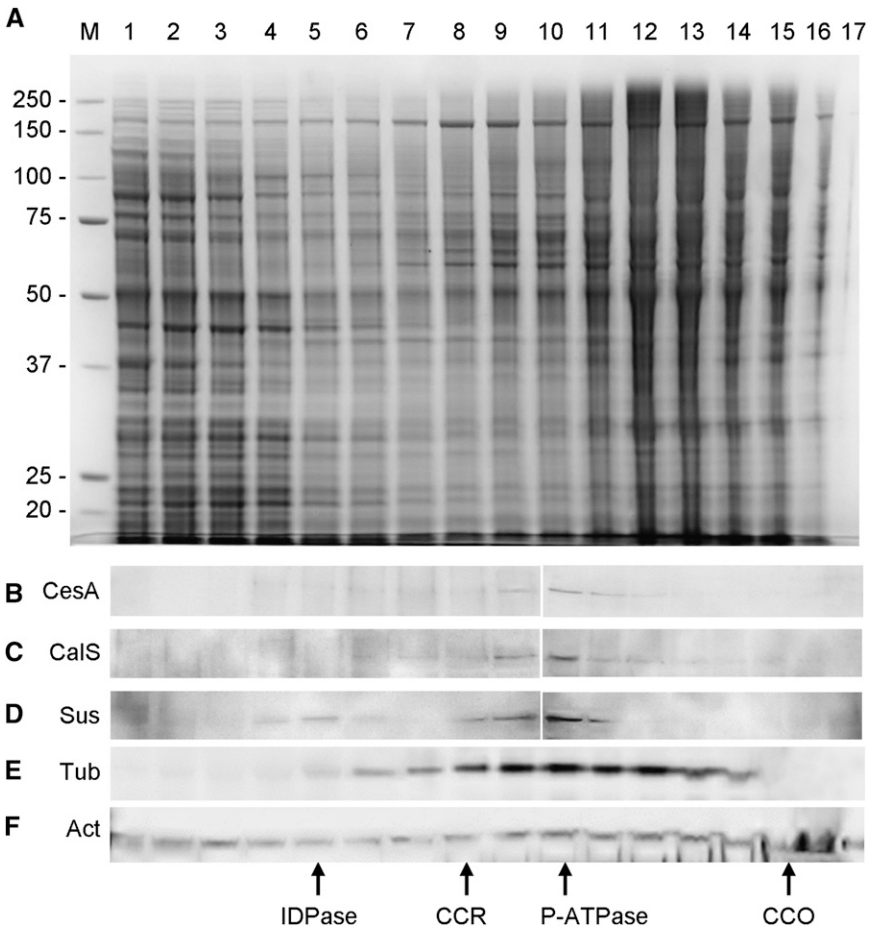

Figure 6. Suc density gradient fractionation of pollen tube membranes. A, The microsomal fraction from 9-h-grown tobacco pollen tubes was centrifuged along 8% to 65% continuous Suc gradients and separated into approximately 20 fractions. Only 17 out of 20 fractions are shown on the SDS-PAGE gel (fraction 1 corresponds to 8% Suc, and fraction 17 corresponds roughly to 57% Suc). Molecular mass markers in kD (M) are on the left. Equivalent volumes were loaded. B, Immunoblot with anti-CesA antibody on the same fractions. The 125-kD band is found in fractions 8 to 13. C, Immunoblot with HDA antibody, which detected CalS in fractions 8 to 12. D, Immunoblot with K2 antibody against Sus; the enzyme peaked around fractions 8 to 12, while a small secondary peak was found in fractions 4 and 5. E, Immunoblot with anti-tubulin antibody showing the distribution of pollen tubulin. F, Immunoblot with anti-actin antibody. The positions of enzyme markers specific for different cellular compartments are also indicated: inosine-5′-diphosphate (IDPase) for Golgi membranes, cytochrome *c* reductase (CCR) for endoplasmic reticulum, P-ATPase for plasma membrane, and cytochrome *c* oxidase (CCO) for mitochondria.

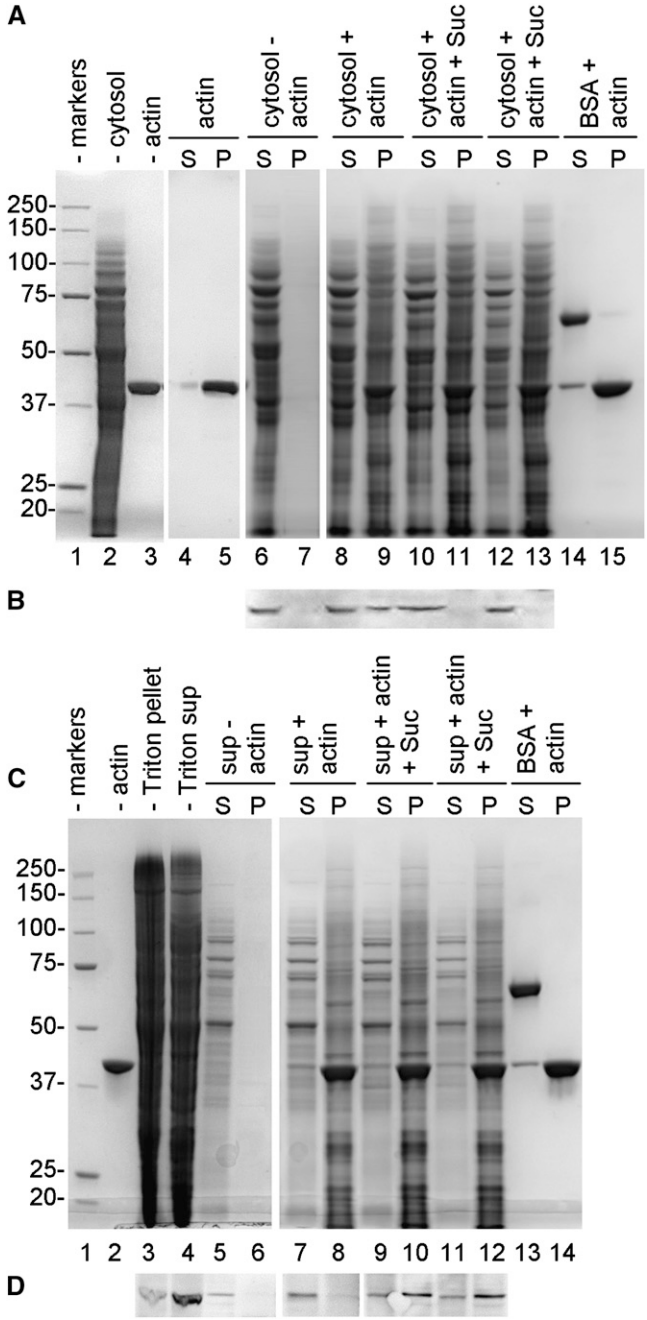

Figure 7. Binding assay of Sus to actin filaments. A, Binding of cytoplasmic Sus. Lane 1, Molecular mass markers; lane 2, cytosolic proteins of pollen tubes (20 μg); lane 3, actin filaments (5 μg). When samples were incubated and centrifuged (S, supernatant; P, pellet), F-actin alone was essentially found in the pellet (lane 5) in comparison with the supernatant (lane 4). Conversely, cytosolic proteins alone were found in the supernatant (lane 6) but not in the pellet (lane 7). Cytosolic proteins were mixed with actin in the absence (lanes 8 and 9) or in the presence of 40 mM Suc (lanes 10 and 11) or 100 mM Suc (lanes 12 and 13). As a control, BSA was also mixed with actin filaments (lanes 14 and 15). B, Immunoblot with anti-Sus on some of the fraction shown in A. Sus was found in the unsedimented cytosolic proteins (lane 6) and in association with actin filaments in the absence of Suc (lane 9) but not in the presence of either 40 or 100 mM Suc (lanes 11 and 13). C, Binding of membrane Sus. Lane 1, Molecular mass markers. Triton-extracted proteins (lane 4; 20 μg) were mixed with actin filaments (lane 2; 5 μg) and centrifuged (S, supernatant; P, pellet). When actin filaments were omitted, membrane proteins did not sediment (lane 6). Membrane proteins were incubated with actin filaments in the absence of Suc (lanes 7 and 8) and in the presence of either 40 mM Suc (lanes 9 and 10) or 100 mM Suc (lanes 11 and 12). As a control, BSA was also mixed with actin (lanes 13 and 14). D, Immunoblot with anti-Sus on the fractions shown in C. Sus was found in the Triton-extracted protein fraction (lane 4), but it did not sediment in the absence of actin (lane 6). Sus did not sediment as well in the absence of Suc (lane 8), but it pelleted with actin in the presence of either 40 mM Suc (lane 10) or 100 mM Suc (lane 12). Blots in D are from the same nitrocellulose membrane.

The behavior of membrane Sus was different (Fig. 7C). Triton-extracted proteins of pollen tubes (lane 4) were mixed with AFs (lane 2) and incubated in the absence of Suc (lanes 7 and 8) and in the presence of either 40 mM Suc (lanes 9 and 10) or 100 mM Suc (lanes 11 and 12). After centrifugation, immunoblots with anti-Sus (Fig. 7D) showed the presence of membrane Sus in the Triton-extracted protein fraction (lane 4) and consistently in the actin pellets obtained in the presence of either 40 mM Suc (lane 10) or 100 mM Suc (lane 12). On the contrary, membrane Sus did not sediment (or poorly) with AFs in the absence of Suc (lane 8). As expected, Sus did not sediment in the absence of AFs (Fig. 7D, lane 6). These data indicate that the rise of Suc concentration abolished the binding of cytoplasmic Sus to AFs while increasing progressively the affinity of membrane Sus to AFs and suggest that the availability of Suc affects the distribution of Sus. Again, in control samples, BSA was unable to bind to AFs in either the absence (Fig. 7C, lanes 13 and 14) or the presence of 40 and 100 mM Suc.

On the other hand, Sus did not bind to MTs and the binding was not affected by Suc concentration (Fig. 8, A and B). Cytosolic proteins did not pellet in the absence of MTs (Fig. 8A, lanes 4 and 5), while tubulin prominently sedimented (lanes 6 and 7). When mixed with MTs, part of the cytosolic proteins bound to MTs and sedimented (lanes 8 and 9), but Sus was still found in the supernatant (Fig. 8B, blot of lanes 8 and 9). Addition of Suc to the mix did not allow Sus to associate with MTs and to sediment (Fig. 8A, 40 mM Suc in lanes 10 and 11, 100 mM Suc in lanes 12 and 13). The behavior of Sus was similar to that of BSA, used as a control for non-MT-binding protein (lanes 14 and 15). Like cytoplasmic Sus, membrane Sus did not bind to MTs under any Suc concentration (the result is practically equivalent to cytoplasmic Sus and therefore is not shown).

To test further the putative interaction between cytoskeleton components (AFs and MTs) and the studied enzymes (Sus, CalS, and CesA), Blue Native-PAGE was used to separate native protein complexes of the plasma membrane of tobacco pollen tubes (Fig. 8C). After separation in the first dimension according to the native molecular mass and in the second di-

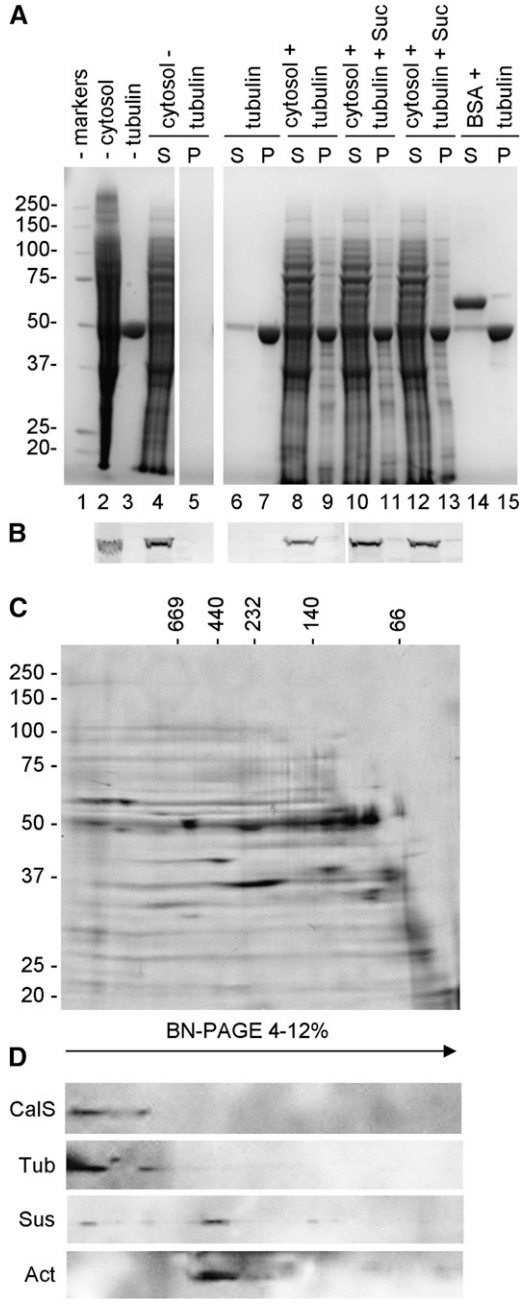

Figure 8. Binding of cytoplasmic Sus to microtubules and analysis of CalS complex by Blue Native-PAGE. A, SDS-PAGE of the binding assay of Sus to microtubules. For clarity, the content of lanes is explained together with information for B. S, Supernatant; P, pellet. B, Immunoblot with anti-Sus on some of the fractions shown in A. Lane 1, Molecular mass markers. Cytosolic proteins (lane 2; 20 μg) assayed in the absence of microtubules (lane 3; 7 μg) did not sediment (lanes 4 and 5). When microtubules were added in the absence of Suc (lanes 8 and 9), part of cytosolic proteins bound to MTs and sedimented but Sus was still found in the supernatant (B, lanes 8 and 9). The presence of Suc in the mix did not allow Sus to sediment with MTs (40 mM Suc in lanes 10 and 11, 100 mM Suc in lanes 12 and 13). The behavior of Sus was similar to that of the control protein BSA (lanes 14 and 15). Lanes 6 to 7, Control of microtubule sedimentation activity. All lanes in A are from the same gel. C, Blue Native-PAGE of plasma membrane proteins separated according to their native molecular mass along 4% to 12% gels (horizontal axis) and then by standard SDS-PAGE on 10% gels (vertical axis). Standards of native molecular mass are indicated on top, while SDS-PAGE standards are indicated on the left. D, Immunoblot with antibodies to CalS, tubulin, Sus, and actin showing their relative migration after Blue Native (BN)-PAGE. Tubulin and CalS cosedimented in a higher molecular mass region around 1,600 kD, while Sus and actin cosedimented around 500 kD.

mension by standard SDS-PAGE, CalS appeared in a protein complex with an approximate mass of 1,600 kD (Fig. 8D, CalS). Tubulin apparently comigrated with CalS in the high molecular mass complex through a physical interaction sufficiently strong to remain during protein isolation. On the other hand, Sus was found to migrate in a protein complex with a mass of around 500 kD (Sus), which also contained actin. Immunoreactivity of Sus was also found in spots around 140 kD (possibly a dimer) and, more interestingly, in higher molecular mass complexes comigrating with CalS and tubulin. These data indicate that Sus can be found at various locations in the pollen tube plasma membrane, mainly in association with actin but also probably with CalS; however, actin did not bind to CalS. Unfortunately, CesA was not detected by immunoblot; consequently, it was not possible to establish its association with other proteins.

Inhibitors of Cytoskeleton and Membrane Dynamics Affect Differently the Distribution of CalS, CesA, and Sus in the Pollen Tube

The aim of this work was to determine the distribution of CalS, CesA, and Sus in relation to cytoskeleton dynamics and endomembrane trafficking. In order to monitor the distribution of vesicles in the tube apex during inhibitory experiments, we took advantage of tobacco plants expressing GFP-labeled Rab11b, a GTPase present in vesicles (de Graaf et al., 2005). The distribution of CalS, CesA, and Sus and the endomembrane trafficking were analyzed using the drug brefeldin A (BFA), which affects membrane trafficking via release/inactivation of Golgi body coat proteins (Nebenführ et al., 2002). The consequences of MT depolymerization and stabilization were analyzed using oryzalin and taxol, respectively (Aström, 1992; Astrom et al., 1995; Gossot and Geitmann, 2007). The role of myosin was investigated using the inhibitor 2,3-butanedione monoxime (BDM), which is known to block myosin activity (Tominaga et al., 2000), while the effect of AF depolymerization was analyzed using latrunculin B (LatB; Cárdenas et al., 2008).

In untreated pollen tubes, GFP:Rab11b-containing vesicles were mainly present in the tube apex in the typical inverted cone shape; Golgi bodies with vesicles move toward the tip in the pollen tube cortex and turn back in the tube center, leaving the vesicles in the apex. BFA induced an accumulation of membranes in the subapical region, generating the so-called BFA mem-

brane compartment (Fig. 9A, arrow in BFA panel). LatB caused a progressive dispersion of the GFP:Rab11b-containing vesicles and thus disappearance of the inverted cone. Inhibition of myosin activity by BDM caused a progressive stop of organelle movement and a uniform dispersion of the GFP:Rab11b-containing vesicles along the pollen tube, confirming that myosin activity is critical for focusing vesicles in the pollen tube apex. Oryzalin and taxol caused only slightly perceptible effects on the distribution of the GFP:Rab11b-containing vesicles. Oryzalin generated a more rounded shape of the vesicular cone, while taxol caused the tail of the vesicle cone to extend farther from the cell tip.

In comparison with controls (Fig. 2), BFA induced a progressive accumulation of intracellular deposits of CalS in distal regions (Fig. 9B, arrowhead in BFA panel), showing that the enzyme is located in the endomembrane system. The apical accumulation of CalS was maintained to a lesser extent (for a time-course experiment, see Supplemental Fig. S3A). LatB affected the apical distribution of CalS already considerably after 15 min (Fig. 9B, LatB top panel) and more pronouncedly after 30 min (bottom panel), with CalS appearing in the rest of the cytoplasm (for a time course experiment, see Supplemental Fig. S3B). Both changes are expected, since we showed that the enzyme is in the endomembrane system. Inhibition of myosin activity by BDM treatment caused CalS to accumulate to a lesser extent in the apical domain and to disappear progressively from distal regions of pollen tubes, leading to the loss of the three-patterned organization. After a 30-min treatment (Supplemental Fig. S3C), the apical cortical distribution of CalS changed into a dispersed intracellular organization. Therefore, the actin-myosin activity influences the transport and accumulation of CalS. Oryzalin and taxol had more specific effects: in the presence of oryzalin, the apical distribution of CalS was relatively unaffected but the organization of CalS in distal regions was dramatically disturbed, with the appearance of consistent intracellular deposits (asterisk in the time course experiment of Supplemental Fig. S3D). Taxol showed comparable effects: the apical accumulation of CalS was maintained but distal cortical CalS disappeared in conjunction with cytoplasmic labeling (asterisk); the taxol effect is also clear in time course experiments (Supplemental Fig. S3E). These data show that MTs are involved in the distribution of CalS in distal regions and, since taxol has this effect, not the presence but the dynamics of MTs are required. All the above-mentioned results were consistently observed (at least five independent experiments each). To determine quantitatively the changes in CalS accumulation, the pollen tube was divided in 10-μm increments along its length and the fluorescence intensity resulting from different assays was measured in each region. As observed in the line graph of Supplemental Figure S4, CalS accumulated significantly in the cytoplasm after BFA treatment but more consistently after treatment with either taxol or oryzalin. Interestingly, the two accumulation areas do not overlap: the BFA-dependent accumulation increased markedly in the region 80 to 90 μm behind the apex and then dropped down; by contrast, the taxol/oryzalin-dependent accumulation was found around 100 to 120 μm behind the apex, where the first callose plug is expected to be formed.

Treatment with inhibitors had different effects on the distribution of CesA proteins (Fig. 9C). In comparison with controls (Fig. 5B), a clear change in CesA distribution was revealed after treatment with BFA: the drug caused a progressive and consistent intracellular accumulation of CesA in the cytoplasm of distal regions (arrow) and a concomitant decrease of CesA in the apical region (asterisk). This change is more evident in time-course experiments (Supplemental Fig. S5A) and shows that CesA travels through the endomembrane system. Treatment with LatB caused the disorganization of AFs in the apical and subapical regions of pollen tubes (Fig. 9E); consequently, the drug induced a progressive redistribution of CesA. Unlike the effect on CalS, LatB produced a progressive relocation of CesA rather than a disappearance (Supplemental Fig. S5B). When the myosin inhibitor BDM was used, CesA persisted in the apical/subapical regions but fluorescence intensity was lower (for a time-course experiment, see Supplemental Fig. S5C). The MT-depolymerizing drug oryzalin, at a concentration that caused complete depolymerization of MTs (Fig. 9F), caused no significant changes in the distribution of CesA, and the enzyme appeared again more concentrated in the apex/subapex. Taxol treatment showed no significant effects as well: the pattern of CesA proteins was relatively comparable to controls, suggesting again that MTs were not critical for CesA distribution (for time-course experiments, see Supplemental Fig. S5, D and E). When the fluorescence intensity of CesA after oryzalin and LatB treatment was measured, results confirmed that the distribution of CesA was unaffected by oryzalin (Supplemental Fig. S6A); although the signal in the apical dome was weaker than the control, the slope of intensity was unchanged. On the other hand, treatment with LatB caused a progressive redistribution of CesA (Supplemental Fig. S6B).

Treatment with inhibitory drugs altered the distribution of Sus; in untreated tubes, Sus was mainly found in the apical cortical cytoplasm and to a lesser extent along the pollen tube shank (Fig. 9D, control). As already shown (Persia et al., 2008), BFA induced the progressive disappearance of Sus from the shank and its accumulation in the tube cytoplasm, suggesting that membrane dynamics are required for the delivery of Sus to the apical membrane and for the maintenance of Sus in the tube shanks. Indeed, also after treatment with LatB, Sus progressively disappeared from the apical region and accumulated consistently in the tube shank; signal also extended progressively into the tube cytoplasm. Apparently, an intact apical actin cytoskel-

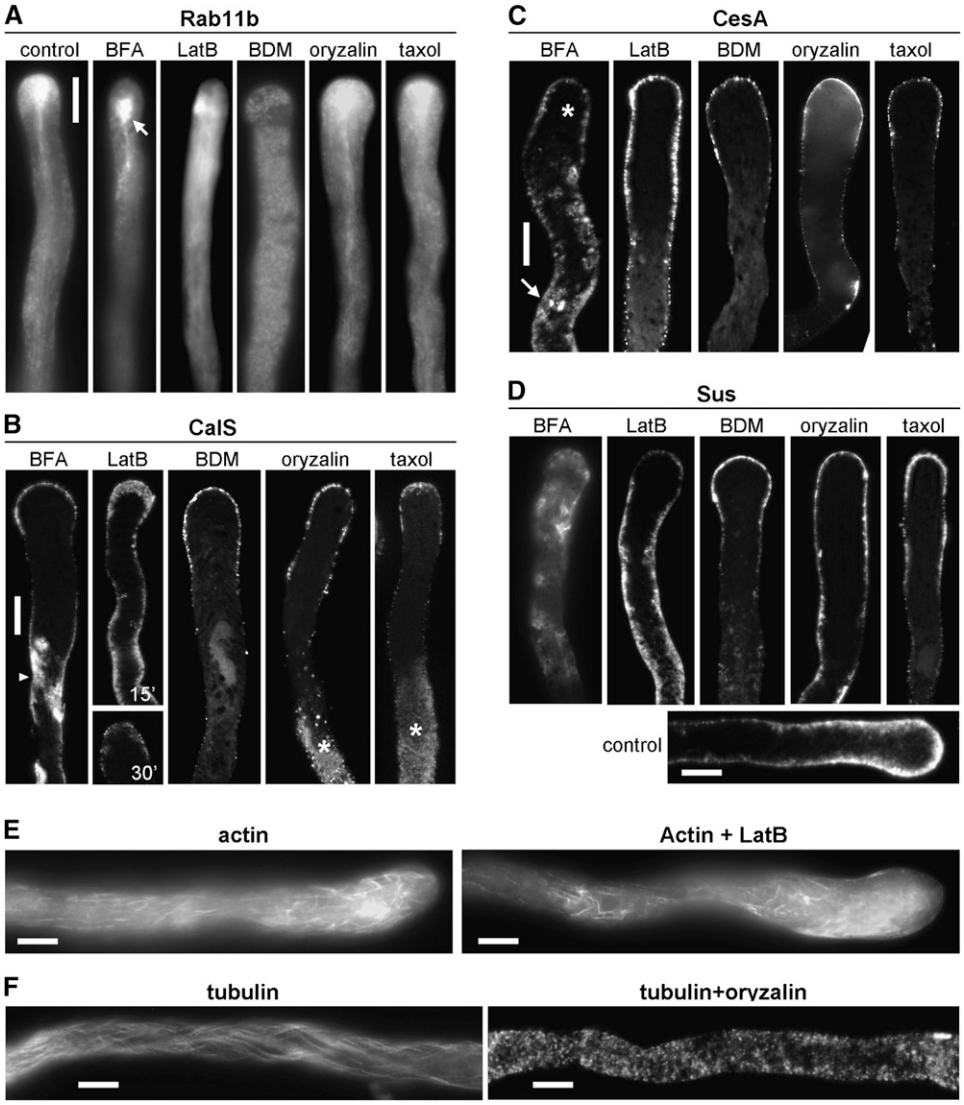

Figure 9. Distribution of apical vesicles, CalS, CesA , and Sus after treatment with inhibitors. Vesicles were visualized in tobacco plants expressing a GFP-labeled Rab11b, while CalS, CesA, and Sus were visualized in wild-type tobacco plants. Experimental conditions were as follows: 5 μg mL^{-1} BFA, 2 nM LatB, 30 mM BDM, 1 μM oryzalin, and 10 μM taxol. A, GFP-labeled Rab11b showing the distribution of apical vesicles (the arrow in the second image indicates the BFA-induced membrane compartment). Bar = 10 μm. B, Distribution of CalS after treatment with inhibitors. BFA caused the accumulation of intracellular deposits of CalS (arrowhead), probably corresponding to BFA-induced aggregates. The three-patterned distribution of CalS was maintained but was less apparent. LatB affected significantly the distribution of CalS after 15 min (top panel) and more strongly after 30 min (bottom panel), causing a uniform distribution of CalS in the cortical region and the disappearance of the strong deposits in the apex. BDM treatment allowed the persistence of lower levels of CalS in the apex but removal of CalS in more distal regions of pollen tubes. Oryzalin and taxol did not interfere with the apical distribution of CalS but generated the progressive disappearance of the distal labeled area and the accumulation of intracellular deposits (asterisks). Bar = 10 μm. C, Effects of inhibitors on the distribution of CesA. BFA induced the accumulation of labeling in the cytoplasm and a consistent decrease in the apical region of pollen tubes (asterisk). LatB induced a progressive relocation of the CesA signal toward basal regions, although labeling was still organized as a tip-base gradient. The myosin inhibitor BDM caused a decrease in the accumulation of CesA in the apical/subapical regions and the progressive disappearance of CesA in distal regions. Oryzalin and taxol caused no significant changes in the distribution of CesA, which was detected according to the tip-base gradient. Bar = 10 μm. D, Effects of inhibitors on the distribution of Sus. BFA induced the progressive disappearance of Sus from the tube shanks and its accumulation in the cytoplasm. LatB induced the progressive disappearance of Sus in the apical domain and accumulation in the base region, with signal that gradually occupied the tube cytoplasm. BDM treatment caused the persistence of an evident staining in the apex but a progressive disappearance or absence in the shanks of pollen tubes. Oryzalin and taxol did not have significant effects on the distribution of Sus. The control pollen tube showed the typical cortical distribution of Sus, with more intense signal in the apex. Bar = 10 μm. E, Effects of the AF inhibitor LatB. In control pollen tubes (left panel), AFs are typically organized as bundles in distal regions and as a network in the subapical domain. After treatment with LatB (right panel), bundles of AFs are still present distally

eton is necessary for the proper delivery of Sus to the apex. Inhibition of myosin activity by BDM did not affect the presence of Sus in the apical region; however, unlike in control pollen tubes, the enzyme was scarcely found in the shank of BDM-treated pollen tubes. This suggests that myosin takes part in the distribution of Sus in the tube shanks but not in the apex. Oryzalin did not alter significantly the pattern of Sus, which was still located in the cortex of both apex and tube shanks. Comparable results were obtained in the presence of taxol; accumulation of Sus in the apical domain and in the tube shanks did not show significant differences from the control. Figure 9E (right panel) shows that oryzalin had induced the disappearance of MTs, leaving only fluorescent spots (unpolymerized tubulin). The addition of taxol, which is known to stabilize MTs, did not affect the MT lattice visibly.

DISCUSSION

In this paper, we show that two fundamental enzymes, CalS and CesA, which are required for the synthesis of cell wall callose and cellulose, respectively, do not distribute uniformly in the pollen tube plasma membrane and that their localization is controlled by AFs and cortical MTs in different ways. Both enzymes are present in the pollen tube apex, suggesting that they deposit callose and CMFs in the pollen tube tip, where CMFs have been reported to occur (Kroh and Knuiman, 1982). A remarkable proportion of CalS is present in distal regions of pollen tubes where callose plugs are being formed and around developing callose plugs; distribution of CalS in distal regions, and therefore in the area where callose plugs are formed, seems primarily dependent on MTs, while we did not find a dependence of CesA distribution on MTs. We further show that cytoplasmic and membrane Sus bind differently to AFs depending on the Suc concentration.

Actin Filaments Control the Overall Distribution of CesA, CalS, and Sus in Pollen Tubes

In pollen tube rosettes, the CesA-containing complexes (Kimura et al., 1999) have been shown by freeze fracturing (Reiss et al., 1985). Cellulose microfibrils may play a critical mechanical role in the apical/subapical region by influencing the diameter of the growing tube (Kroh and Knuiman, 1982, 1985; Aouar et al., 2010). Two potential CesA genes have been identified in the pollen tube of *N. alata*. The NaCslD1 gene is highly expressed in pollen, but it is unclear if the gene codes for the "real" CesA of pollen tubes; in fact, the so-called "cellulose synthase-like" (Csl) genes are structurally related genes of unknown function that have been hypothesized to participate in the synthesis of noncellulosic polysaccharides (Richmond and Somerville, 2000). However, NaCslD1 contains all the regions typical of plant CesA proteins, such as the homology domains H-1, H-2, and H-3, the plant-conserved region, and the hypervariable region; the D,D,D,QVLRW motif is also present in the NaCslD1 sequence (Pear et al., 1996). The second gene (NaCesA1) is not expressed (or expressed at a very low level) in pollen tubes; therefore, its role in the synthesis of cellulose is questionable. Since CesA sequences (and proteins) have not been clearly identified in the pollen tube of tobacco, we used an antibody raised against a conserved peptide sequence (NELPRLVYVSREKRPG) that is present in both the real nonexpressed NaCesA1 and in the NaCslD1 sequence (although with less homology). The antigenic peptide sequence is also present in the cellulose synthase-like protein CslE (GenBank accession no. AAZ32787.1) and in the cellulose synthase-like protein CslG (GenBank accession no. AAZ79231.1) of tobacco.

Although the biochemistry and subcellular localization of CalS in pollen tubes are relatively known, the relationship between CalS, the cytoskeleton, and membrane dynamics has not been reported. We found the 225-kD CalS polypeptide mainly in association with the plasma membrane and cell wall protein fractions of tobacco pollen tubes. Most of the labeling is associated with the plasma membrane or with the first nanometers of the cell wall facing it. Assuming the scale and dimension of gold particles (15 nm) and of the two antibodies used for indirect immunolabeling, a putative distance between the antigen and the center of gold particles can be estimated around 30 nm (Kimura et al., 1999), but the presence of CalS in the cell wall could also be caused by the fixation method used. However, localization of CalS in the plant cell wall is not unexpected (Ian et al., 1998) and is also further supported by immunoblotting on different protein fractions from tobacco pollen tubes. The localization of tobacco CalS is consistent with its role in callose production (Brownfield et al., 2008).

We tested whether apart from membrane trafficking an intact AF cytoskeleton is required for the maintenance of CesA and CalS in the apical region. As expected for a plasma membrane protein, BFA accumulated both proteins in intracellular membrane compartments. The BFA experiments together with electron microscopy images show that they travel to the plasma membrane of the pollen tube tip via Golgi membranes. The AF-depoly-

Figure 9. (*Continued.*)
but the subapical network disappears. Images are single cortical optical sections. Bars = 10 μm. F, Effects of the MT inhibitor oryzalin on the organization of MTs in the pollen tube. In controls (left panel), MTs show the typical filamentous arrangement, which is lost after treatment with oryzalin (right panel), leaving only diffused fluorescent spots. Images are whole cell projections. Bars = 10 μm.

merizing drug LatB, which caused disappearance of the subapical actin fringe, retraction of AF bundles in the pollen tube shank, and growth arrest (Cárdenas et al., 2008), relocates the enzymes progressively backward along the tube shank, showing that a proper organization of AFs is critical for the distribution of CesA and CalS. The appearance of intracellular deposits after BFA treatment is similar to the accumulation of ARA7-labeled endosomes as observed in Arabidopsis pollen tubes (Zhang et al., 2010), suggesting that the distribution of these enzymes is also dependent on a recycling mechanism, as has been suggested for CesA by Crowell et al. (2009). The role of AFs is confirmed by immunocytochemical evidence of the enzymes in association with vesicular structures close to the plasma membrane (Fig. 5, H and I) and by treatment with BDM, which disturbs myosin. Although BDM is reported to cause broad effects in plant cells (such as on AFs, cortical endoplasmic reticulum, and the MT cytoskeleton; Samaj et al., 2000), current and other reports suggest that cellulose (Wightman and Turner, 2008; Crowell et al., 2009; Gutierrez et al., 2009) and callose (Chaffey and Barlow, 2002) synthesis require an acto-myosin mechanism. BDM does not remove the CesA and CalS already there from the plasma membrane, as is expected. In addition, labeling is retained in the pollen tube apex, where the vesicles are located. The different results with LatB, which clears the apex from vesicle label (Fig. 9A), indicate that myosin transports the Golgi bodies to the subapex but not the Golgi vesicles from there to the plasma membrane of the pollen tube tip. Actin-myosin interactions appear to be important for the delivery of the enzymes to the pollen tube subapex through Golgi bodies, but Golgi-derived secretory vesicles may not depend on this system.

The reaction of organelle and vesicle distribution to MT inhibitors indicates that MTs do not take part in the delivery of the enzymes to the pollen tube apex. This evidence is consistent with data indicating that MTs are not critical for the transport of Golgi bodies with secretory vesicles to the pollen tube apex (Cai and Cresti, 2009, 2010). Analysis of the behavior of yellow fluorescent protein fused to CesA in transgenic Arabidopsis cells showed that AFs transport CesA-containing Golgi bodies and deliver them to sites of cell wall synthesis (Wightman and Turner, 2008). The process of CSC insertion into the plasma membrane takes place preferably in association with MTs (Gutierrez et al., 2009), although without MTs the insertion of CSCs goes on at the same rate as before drug application (Gutierrez et al., 2009). A specific CesA-associated membrane compartment, called the small CesA-containing compartment (Gutierrez et al., 2009) or membrane compartments associated with MTs (Crowell et al., 2009), was observed to move along depolymerizing cortical MTs from which CesA insertion into the plasma membrane took place (Gutierrez et al., 2009). Distribution of CesA in pollen tubes is maintained after treatment with either taxol or oryzalin, and we did not find a significant colocalization of CSCs with MTs. However, we did find aligned CSCs, suggesting that part of them align along MTs. MTs are hardly detected in the apex, although the use of GFP-AtEB1 revealed the presence of dynamic MTs within the apical domain (Cheung et al., 2008). Therefore, MTs could regulate the insertion of the membrane containing these enzymes in a small defined area in order to regulate the growth of pollen tubes. The interactions between MTs and CSCs should be further studied in more detail in living pollen tubes.

The evidence that MT inhibitors (taxol and oryzalin) had no dramatic effects on Sus distribution (coupled with the finding that Sus did not bind to MTs and MTs did not comigrate with Sus in Blue Native-PAGE) shows that the localization of Sus is mainly controlled by AFs. Distribution of Sus in the plasma membrane is dependent on the activity of Golgi membranes, as shown by immunodetection of Sus in a Golgi marker-enriched vesicle fraction and by the disorganization of Sus distribution after BFA treatment (Persia et al., 2008; this paper). This finding is comparable with the one proposed to operate in maize, where Sus is enriched in the Golgi system and plasma membranes and is likely to be involved in the delivery of substrates to β-glucan synthase and cellulose synthase (Buckeridge et al., 1999).

Microtubules Control the Localization of CalS for Callose Plug Formation in Pollen Tubes

CalS is abundantly present in distal regions of the pollen tube. A local higher amount of CalS is expected to be involved in the synthesis of callose plugs, which is further supported by an increasing concentration of CalS around developing callose plugs. Distal CalS is slightly affected by LatB treatment, indicating that the mechanism of delivery and accumulation also relates to AFs. MTs appear to be significantly involved in the distribution and maintenance of distal CalS. Association of MTs with CalS is also supported by Blue Native-PAGE experiments, which indicate that MTs (but not AFs) can directly bind to CalS. Our data are in agreement with previous observations by Blue Native-PAGE performed in tobacco BY-2 cells (Aidemark et al., 2009). The Blue Native-PAGE experiment suggests that insertion of CalS in the plasma membrane requires the interaction of MTs with membrane-associated CalS. The drug-mediated removal or stabilization of MTs indeed prevents the correct localization of CalS. Also in BY-2 cells, treatment with oryzalin was shown to affect callose deposition (Aidemark et al., 2009). Current experiments with taxol suggest that the dynamics of MTs rather than their presence is critical for the correct localization of distal CalS.

In longer tubes, CalS is present at the borders of growing callose plugs while MTs remain more or less longitudinal to the tube's long axis; this suggests that MTs could continuously promote plug growth by either repositioning the preexisting CalS at the border of the growing plug or adding new CalS molecules via vesicle delivery. The current literature indicates that an

intact MT cytoskeleton is required for CalS activity in Arabidopsis and tobacco BY-2 cells (Aidemark et al., 2009), while the synthesis of callose in the liverwort *R. helicophylla* was supposed to depend on the binding of CalS to cortical MTs (Scherp et al., 2002). In pollen tubes of tobacco, depolymerization of MTs by oryzalin caused a considerable reduction in the number of callose plugs, indicating that MTs are important for the proper synthesis of callose in the plugs (Laitiainen et al., 2002). On the basis of past and current observations, we propose the following model (Fig. 10). CalS is synthesized in the endoplasmic reticulum and via Golgi bodies is transported toward the subapex along AFs. The Golgi-derived vesicles then move to the apex, a process that possibly does not involve myosin. Then, the membrane of Golgi vesicles containing CalS is inserted into the apical plasma membrane, where CalS starts to produce callose. In the subapex, CalS is removed by endocytosis and eventually recycled; the enzyme also might be deactivated (as suggested by Brownfield et al., 2008). Distally, AFs distribute Golgi bodies and CalS is inserted into the plasma membrane by a process mediated by MTs; this hypothesis is supported by evidence that in oryzalin-treated tubes, the number and position of callose plugs are substantially altered (Laitiainen et al., 2002). Interestingly, the third segment of CalS appears around 100 μm from the tube tip (Fig. 2D); the synthesis of callose plugs is supposed to start in defined areas of the plasma membrane where no net flux of H^+ occurs (Certal et al., 2008), the first being around 100 μm from the tube tip. The effects of taxol and oryzalin are rather specific for CalS, because these drugs caused no significant changes in the distribution of either CesA or Sus. At the border of developing plugs, the presence of Sus increased considerably, indicating that Sus is required for the formation of callose plugs, as expected. Unsurprisingly, CesA did not accumulate in the callose plugs, which supports the evidence that cellulose is not present in the plugs (Ferguson et al., 1998) but only in the original cell wall before plug formation.

Cytoplasmic and Membrane Sus Bind Differently to AFs Dependent on the Suc Concentration

Sus is a fundamental enzyme that provides activated metabolites to CalS and CesA and therefore potentially controls the synthesis of cellulose and callose (Amor et al., 1995). The regulatory role of Sus is most likely achieved by finely tuning its partition between a cytoplasmic form (not involved in the synthesis of cell wall polysaccharides) and a membrane-binding form (possibly associated with CesA and CalS). Factors controlling such a distribution are therefore capable of regulating cell wall synthesis. Phosphorylation of critical amino acids is one mechanism that possibly regulates the binding of Sus to the plasma membrane (Hardin et al., 2004); other candidates are the concentration of Suc and the affinity to AFs (Duncan and Huber, 2007). In a previous paper (Persia et al., 2008), the availability of external Suc was shown to affect the intracellular distribution of Sus in the pollen tube. When Suc in the germination medium was replaced by glycerol (a nonmetabolizable compound), Sus was found at very low levels in the plasma membrane and cell wall fractions but at higher levels in the cytoplasm. In this work, we show that cytoplasmic and membrane Sus bind differently to AFs in the presence of variable Suc concentrations. These and past results (Duncan and Huber, 2007) suggest that Sus associates prevalently with the plasma membrane in the presence of high Suc levels. Such an association is probably supported by dephosphorylation (Persia et al., 2008) and the binding of membrane Sus to AFs and could be a general

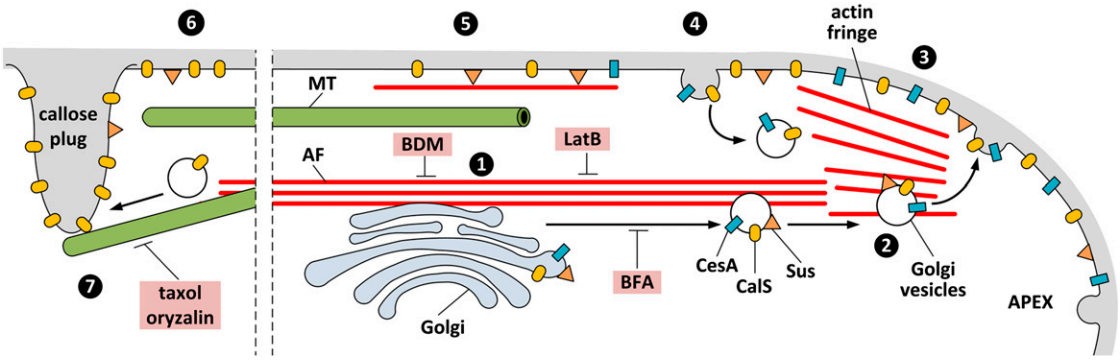

Figure 10. Schematic drawing showing the current hypothesis about CalS/CesA insertion into the pollen tube plasma membrane. CalS and CesA are synthesized in the endoplasmic reticulum (data not shown) and in Golgi bodies transported to the subapex along bundles of actin filaments (1), from where Golgi vesicles to which Sus also is associated (2) move to the apical plasma membrane where the vesicle membrane is inserted, including the enzymes (3). In the subapex, the excess of CalS and CesA is removed by endocytosis and may be eventually recycled (4). Accordingly, a smaller proportion of CalS and CesA persists in the tube (5), although new insertion of CesA make take place here. Sus might associate with cortical actin filaments, which are used to establish the correct spatial arrangement. Additional CalS, but not CesA, is inserted into the plasma membrane where a callose plug is formed (6), the localization of which is determined by microtubules (7). The targets of the inhibitors used are indicated. Objects are not drawn to scale. Dotted lines indicate that the distance between the apex and the first callose plug is larger than shown.

requirement for the interaction of Sus with either CesA or CalS for the synthesis of cell wall polysaccharides (Salnikov et al., 2001). In this hypothesis, a decrease of Suc concentration reduces the affinity of membrane Sus for AFs. Given that the Suc concentration also affects the binding of Sus to the plasma membrane (Duncan and Huber, 2007; Persia et al., 2008), the decrease of the Suc concentration induces the conversion of Sus into the cytoplasmic form. Conversely, the increase of the Suc concentration induces the conversion of Sus into the membrane form, which might bind to AFs and initiate the formation of a multiprotein complex that facilitates cellulose/callose synthesis.

MATERIALS AND METHODS

Production of Antibodies to CalS

Amino acid sequences of CalS from *Nicotiana alata* (NaGSL1; GenBank accession no. AF304372.2) and Arabidopsis (*Arabidopsis thaliana*; GSL5; GenBank accession no. AY337762.1) were compared by BLAST (http://blast.ncbi.nlm.nih.gov/Blast.cgi) and ClustalW (http://www.ebi.ac.uk/Tools/clustalw2/index.html) software. We identified 11 peptide sequences, distributed all along the protein backbone, in which homology was identical. Those sequences were assayed for immunogenicity by the private company in charge of antibody production (Primm; www.primm.it). On the basis of the know-how of this private company, several potential immunogenic peptides were identified, and three of them were selected: peptide 1 (amino acids 72–87 of *Nicotiana* CalS) with the sequence NH_2-RVAYLCRFYAFEKAHR-COOH; peptide 2 (amino acids 335–349) with the sequence NH_2-QRKILYMGGLYLLIWG-COOH; and peptide 3 (amino acids 1,394–1,409 of *Nicotiana* CalS) with the sequence NH_2-PLKVRFHYGHPDVFDR-COOH. The first two peptides are present in the N-terminal cytoplasmic domain of CalS (a region that does not belong to the glucan synthase domain) and were used for production of a first antibody (HDA). A second antibody (DDA) was raised against the third peptide, which is present in the large intermediate cytoplasmic fragment of CalS and is part of the 1,3-β-glucan synthase domain (Østergaard et al., 2002). Peptides were synthesized and conjugated to KLH carrier protein and used to immunize rabbits according to the following procedure: sampling of preimmune serum, immunization of rabbits (day 0) with 300 μg of antigen in Complete Freund Adjuvant, second immunization (day 21) with 300 μg of antigen in Incomplete Freund Adjuvant, third immunization (day 28) with 300 μg of antigen in Incomplete Freund Adjuvant, fourth immunization (day 35) with 300 μg of antigen in Incomplete Freund Adjuvant, bleed (day 42) of 500 μL of serum for ELISA test, fifth immunization (day 45) with 150 μg of antigen in Incomplete Freund Adjuvant, and final bleed (40 mL per rabbit). After delivering, antibodies were purified by antigen affinity using proteins bound to nitrocellulose (Olmsted, 1981).

The optimal dilution of anti-CalS antibodies was determined by immunoblot with a multiscreen apparatus from Bio-Rad, while the affinity of antibodies was checked by dot-blot assays. Samples (antigen peptides conjugated to KLH or secondary antibody) were spotted onto nitrocellulose membrane (Bio-Rad) at chosen concentrations and then allowed to dry. The nitrocellulose membranes were transferred to polystyrene square plates and incubated in blocking solution (5% [w/v] blocking agent [GE Healthcare] in Tris-buffered saline [TBS] plus 0.1% [v/v] Tween 20 [TBS-T]) for 1 h at room temperature. The membranes were treated with the rabbit CalS antibody (1:300 in TBS-T), washed three times for 5 min each in TBS, and then incubated with the goat anti-rabbit horseradish peroxidase-conjugated secondary antibody (1:5,000) for 1 h at room temperature. After washing three times for 5 min each in TBS, the membranes were transferred to enhanced chemiluminescence reagents and visualized.

Antibody to CesA

Antibody to CesA was a polyclonal antibody against 15 amino acids (NH_2-NELPRLVYVSREKRPGC-COOH) present in all 10 isoforms of CesA in Arabidopsis (Gillmor et al., 2002). The peptide sequence is also found in the cellulose synthase sequences (CesA1, AAK49454.1; CslD1, AAK49455.1) identified in *N. alata* pollen tubes with identities of 92% and 85%, respectively. The peptide sequence is located in the large central cytoplasmic domain of CesA (Pear et al., 1996). The antibody was kindly provided by Prof. Chris Somerville.

Other Antibodies and Pharmacological Treatments

Antisera to Sus have been already described in a previous paper (Persia et al., 2008), and their specificity will not be further discussed here. Labeling of tubulin was achieved using the antibody B-5-1-2 (Sigma Chemicals), which recognized α-tubulin from different sources, such as bovine brain, tobacco (*Nicotiana tabacum*) leaves, Arabidopsis, and grapevine (*Vitis vinifera*) tissues (Parrotta et al., 2010). A monoclonal anti-plant actin antibody (clone 10-B3) capable of recognizing actin in many plant species was purchased from Sigma.

Inhibitors of cytoskeleton and membrane dynamics were used as already described in other papers. Inhibitors were used at concentrations that interrupt cell activities without producing cell death and were applied 3 h after germination or according to the time-course experiments. LatB was used for 5-10-20 min at 2 nM, a concentration that caused degradation of the cortical actin fringe and disorganization of AFs in the tube shanks (Cárdenas et al., 2008); the effect of LatB on tobacco pollen tubes has been already described (de Graaf et al., 2005). Oryzalin was used for 10-20-40 min at 1 μM, a concentration capable of depolymerizing most MTs in tobacco pollen tubes and other species (Astrom et al., 1995; Gossot and Geitmann, 2007). Taxol was used for 10-20-40 min at 10 μM, a concentration that stabilizes MTs in tobacco pollen tubes (Aström, 1992). BFA was used for 5-10-15 min at 5 μg mL^{-1}, a value that established a stable and dynamic system of membranes in the pollen tube of tobacco and other species (Rutten and Knuiman, 1993; Parton et al., 2003). Myosin activity was inhibited by treatment with 30 mM of the myosin inhibitor BDM for 5-10-30 min (Tominaga et al., 2000); the effects of BDM on tobacco pollen tubes are shown in Supplemental Videos S1 and S2. The effects of cytoskeletal and membrane inhibitors on tobacco pollen tubes were identical to those already described in the literature and are not consequently shown here (except for oryzalin and BDM). All drugs were used from high concentrated stock solution in dimethyl sulfoxide. In control samples, pollen tubes were analyzed after growing in either standard medium or in medium supplemented with the equivalent concentration of dimethyl sulfoxide. No differences were observed.

Analysis of callose and cellulose by staining with aniline blue and calcofluor white, respectively, revealed no critical differences in the distribution of both polymers after treatment with inhibitors (Supplemental Fig. S7). This is not unexpected, because LatB, BFA, and BDM stop pollen tube growth by inhibiting vesicular trafficking, but preexisting cellulose and callose are likely not removed from the plasma membrane. On the contrary, taxol and oryzalin did not affect the growth of pollen tubes, and deposition of new cell wall polymers at the subapex continues.

GFP-Tagged Rab11b-Containing Vesicles

Vesicle trafficking in the pollen tube apex was analyzed by monitoring Rab11b, a member of the Ras superfamily that targets to the apical clear zone of pollen tubes and probably regulates the trafficking of Golgi vesicles to the cell membrane and the transport of recycled vesicles in the pollen tube apex (de Graaf et al., 2005). Stably transformed tobacco plants expressing a GFP-tagged pollen-expressed Rab11b were obtained from Prof. Alice Cheung (Department of Biochemistry and Molecular Biology, University of Massachusetts, Amherst). Seeds were sterilized by washing with 70% (v/v) ethanol (5 min) and with 70% (v/v) bleach with a drop of detergent (5 min). After shaking the tube to mix seeds, the bleach was washed out and seeds were plated on Murashige and Skoog medium with 1% (w/v) Suc and 50 μg mL^{-1} kanamycin (to select the resistant ones). After plant growth and anthesis, pollen tubes were checked for fluorescence, which was localized predominantly to an inverted cone-shaped region in the tube tip. Distribution of Rab11b was used to monitor the tip-focused vesicle trafficking under inhibitory experiments.

Protein Extraction

Proteins from Arabidopsis plants were extracted by selective solubilization in phenol and subsequent precipitation with 0.1 M ammonium acetate in 80% (v/v) methanol (Wang et al., 2006). The method is suitable for the extraction of proteins from a variety of plants (including recalcitrant plants).

Germination of tobacco pollen grains was performed under standard conditions (constant concentrations of pollen, constant temperature of 25°C, and agitation speed set at 50 rpm). Under these settings, the percentage of germinated grains is usually around 80%; nevertheless, we usually count the germinated pollen grains before proceeding. We consider this step as standard; therefore, we do not remove the ungerminated pollen. Proteins were

extracted from cytosol and membranes of pollen tubes according to the method described by Persia et al. (2008). Cell wall proteins of tobacco pollen tubes were extracted following the protocol described by Li et al. (1983) with the modifications introduced by Persia et al. (2008).

Fractionation of Pollen Tube Membranes and Assay of Enzyme Markers

Although 3 h of pollen germination is the standard protocol used in our laboratory, Brownfield et al. (2008) have shown that the concentration of CalS increased considerably after 8 h of growth, during which CalS progressively moved from internal membranes to the plasma membrane. To demonstrate that tobacco CalS is associated with the plasma membrane, therefore, we needed to use pollen grains germinated for long time (more than 9 h). Pollen tubes are usually still alive and growing not only after 9 h but also for a longer time (16–24 h). Organelles of pollen tubes after 9 h of growth were fractionated by centrifugation over a continuous 8% to 65% Suc gradient. Starter Suc solutions at 8% (w/v) and 65% (w/v) were prepared in 50 mM imidazole, pH 7.5, 2 mM EDTA, 1 mM phenylmethylsulfonyl fluoride (PMSF), and 1 mM dithiothreitol (DTT); intermediate Suc solutions at 22.3%, 36.5%, and 50.7% were prepared by mixing appropriately the two starter solutions. Aliquots (2 mL) of each solution (from 65% to 8%) were sequentially added to 13-mL centrifuge tubes using a cut pipette tip. Tubes were allowed to stand overnight at 4°C, thus forming a linear Suc gradient. Alternatively, a gradient former from GE Healthcare was also used. The high-speed pellet obtained previously was dissolved in a resuspension buffer (50 mM imidazole, pH 7.5, 2 mM EDTA, 1 mM PMSF, 1 mM DTT, and 0.1 M Suc), and 1-mL aliquots were loaded over the Suc gradient. Samples were centrifuged at 100,000*g* for 2 h at 4°C. Fractions of 0.5 mL were recovered from each tube using a pipette and then stored at −80°C.

The following enzyme markers were assayed for each fraction: inosine-5′-diphosphatase activity for Golgi vesicles (in the presence and absence of Triton X-100), P-ATPase activity for plasma membrane (in the presence and absence of vanadate), cytochrome *c* reductase activity for endoplasmic reticulum, and cytochrome *c* oxidase activity for mitochondria. Protocols were performed exactly as described in the literature (Turner et al., 1998; Robinson and Hinz, 2001). Enzyme activities were always expressed as percentages of maximum activity. Three different membrane fractionations were used for the analysis of organelle markers. Free inorganic phosphate was determined using the colorimetric assay from Cytoskeleton.

Electrophoresis and Immunoblotting

Electrophoretic analysis of proteins was done using precast Criterion XT gels (Bio-Rad) at 10% acrylamide concentration. The running buffer was XT MOPS, and proteins were separated at 200 V (constant) using a Power Pac power supply. After running, gels were stained with Bio-Safe Coomassie (Bio-Rad). For immunoblot analysis, unstained gels were washed briefly with blotting buffer (25 mM Tris, 192 mM Gly, pH 8.3) and then mounted in the blot cassette of a Criterion blotter (Bio-Rad) in contact with nitrocellulose membranes. Transfer of proteins was achieved at 100 V (constant) for 30 min at 4°C. After blotting, membranes were briefly washed in the transfer buffer and then allowed to air dry. Membranes were blocked overnight in 5% (w/v) blocking agent (GE Healthcare) in TBS-T. Primary antibodies were diluted in TBS-T as follows: 1:300 for antibodies to CalS, 1:1,000 for antibodies to CesA, Sus, and actin, and 1:5,000 for the B-5-1-2 anti-tubulin antibody. Antibodies were incubated for 1 h at room temperature, and excess of antibody was removed by several washes with TBS. Goat anti-rabbit and goat anti-mouse horseradish peroxidase-conjugated secondary antibodies (GE Healthcare) were diluted 1:5,000 in TBS-T and incubated with membranes for 1 h at room temperature. Excess of secondary antibody was removed by several washes with TBS, and the immunological complex was visualized by enhanced chemiluminescence reaction using reagents from GE Healthcare.

Blue Native-PAGE

Separation of plasma membrane proteins by Blue Native-PAGE was achieved according to the method described by Aidemark et al. (2009). Germinated pollen tubes were homogenized in lysis buffer (25 mM HEPES, pH 7.5, 3 mM EGTA, 3 mM EDTA, 2 mM $MgCl_2$, 2 mM DTT, and 10 μL mL^{-1} protease inhibitors) and centrifuged at 7,000*g* for 10 min at 4°C. The pellet was discarded, while the supernatant was centrifuged at 50,000*g* for 60 min at 4°C. The pellet was resuspended in 25 mM HEPES (pH 7.5), 250 mM Suc, 1 mM EDTA, and 1 mM DTT. It was subsequently added to the "two-phase partitioning solution" made of 3.4 g of 20% Dextran T-500, 1.7 g of 40% polyethylene glycol-3350, 2.15 g of HSK (for 25 mM HEPES, pH 7.5, 1 M Suc, and 8 mM KCl) and brought to 9 g with water (Robinson and Hinz, 2001). The solution was vigorously mixed by inverting the tube 40 times. Tubes were centrifuged for 5 min at 1,500*g*, and the upper phase (enriched in plasma membrane) was added to fresh lower phase and mixed vigorously again by inverting the tube 40 times. After centrifugation for 5 min at 1,500*g*, the upper phase was removed and diluted 1:1 with resuspension buffer (25 mM HEPES, pH 7.5, 250 mM Suc, 1 mM EDTA, and 1 mM DTT). This protocol has been used already for characterizing plasma membrane proteins of tobacco pollen tubes (Cai et al., 2005), in which the purity of the plasma membrane fraction was evaluated by P-ATPase activity in the presence and absence of orthovanadate. The resuspended sample was centrifuged for 60 min at 100,000*g*, and the plasma membrane-enriched pellet was extracted with solubilization buffer (0.5 mM EDTA, 500 mM aminocaproic acid, 20% Suc, 50 mM Bis-Tris, 2 mM PMSF, 10 μL mL^{-1} protease inhibitors, 100 mM NaCl, and 2% *n*-octyl-β-D-glucopyranoside). After incubation at 4°C for 30 min, the detergent-insoluble fraction was pelleted at 100,000*g* for 60 min at 4°C. The supernatant was supplemented with Coomassie Brilliant Blue G-250 to a final concentration of 0.8% to 1% (w/v). Samples were loaded in the wells of a 4% to 12% Criterion gel for Blue Native-PAGE, separated at 100 V for 45 min and then at 200 V until the dye front reached the gel bottom (about 5 h at 4°C). The cathode buffer was 50 mM Tricine/15 mM Bis-Tris, pH 7, 0.02% Coomassie Brilliant Blue, while the anode buffer consisted of 50 mM Bis-Tris, pH 7, 250 mM aminocaproic acid. Gel lanes were cut and stored at −80°C. Native standards were from GE Healthcare (thyroglobulin, 669 kD; ferritin, 440 kD; catalase, 232 kD; lactate dehydrogenase, 140 kD; albumin, 66 kD). For the SDS-PAGE second dimension, lanes were thawed and incubated with 1% SDS and 1% β-mercaptoethanol for 15 min and then placed on the top of a 10% Criterion XT gel, run as described above, and stained with Bio-Safe Coomassie. Blue Native-PAGE experiments were done three times, and blot assays were performed comparably.

Immunofluorescence and Immunoelectron Microscopy

Indirect immunofluorescence microscopy was performed on germinated pollen according to Del Casino et al. (1993). Pollen tubes were fixed in 3% paraformaldehyde, 12% Suc in 50 mM PIPES, pH 6.9, 1 mM EGTA, and 0.5 mM $MgCl_2$ for 30 min; after washing, the cell wall was digested with 1.5% cellulysin for 4 min and then pollen tubes were further fixed with cold methanol. Primary antibodies were diluted in PBS as follows: anti-Sus, 1:100; anti-CalS, 1:50; anti-CesA, 1:100; anti-tubulin, 1:500. The following secondary antibodies were diluted 1:150 in PBS: Alexa Fluor 488-conjugated goat anti-rabbit IgG and Alexa Fluor 595-conjugated goat anti-mouse IgG (both from Invitrogen). AFs were stained using Alexa 543-phalloidin according to the chemical fixation method described by Lovy-Wheeler et al. (2005). Observations were made with a Zeiss Axio Imager optical microscope equipped with a 63× objective. Images were captured with an MRm AxioCam video camera using AxioVision software. High-quality images were obtained using the Apotome module. In controls, the primary antibodies were omitted or preimmune serum was used.

Double labeling experiments were performed to visualize simultaneously either CesA or CalS and tubulin; in such cases, the rabbit polyclonal antibodies to CesA/CalS and the mouse monoclonal anti-tubulin primary antibodies were mixed and incubated simultaneously. After washing to remove excess antibodies, the corresponding secondary antibodies were also mixed and applied. Images were acquired and combined using the Multi Channel module of the Zeiss Axio Imager optical microscope.

For immunogold labeling, samples of pollen tubes were fixed in 1.5% formaldehyde and 0.75% glutaraldehyde in phosphate buffer, pH 6.9, for 30 min at room temperature. After fixation, samples were rinsed with phosphate buffer and dehydrated gradually in a series of increasing concentrations of ethanol (from 10% to 100%). Samples were embedded in LR White resin, polymerized for 2 d at 40°C, and then cut into 600-Å sections using a Leica Ultracut R microtome. After sectioning, samples were incubated with 3% normal goat serum in 0.05 M Tris-HCl + 0.2% BSA to block nonspecific immunoreactivity. The anti-CalS and anti-CesA primary antibodies were diluted in PBS at 1:50. The secondary goat anti-rabbit Ig 15-nm gold-conjugated antibody was used at a dilution of 1:50 (BioCell). Sample images were captured with a Philips Morgagni 268D transmission electron microscope operating at 80 kV and equipped with a MegaView II CCD camera (Philips Electronics).

Binding Analysis of Sus to Actin Filaments and Microtubules

Cytoplasmic and membrane proteins of tobacco pollen tubes were obtained as described above in "Protein Extraction." The high-speed pellet was resuspended with 1 mL of solubilization buffer (50 mM imidazole, pH 7.5, 2 mM EDTA, 1 mM DTT, 1 mM PMSF, and 0.1% Triton X-100) and incubated for 1 h at 4°C with constant agitation. After centrifugation at 100,000*g* for 1 h at 4°C, the supernatant (containing solubilized membrane proteins) was then used. For the binding assay to AFs, one aliquot of actin (1 mg) was thawed and diluted to a concentration of 10 mg mL^{-1} by adding 100 μL of A buffer (5 mM Tris-HCl, pH 8.0, 0.2 mM $CaCl_2$, 0.2 mM ATP, and 0.5 mM DTT). Actin was further diluted at a concentration of 0.4 mg mL^{-1} with A buffer and incubated on ice for 1 h. The polymerization inducer (10×: 500 mM KCl, 20 mM $MgCl_2$, and 10 mM ATP) was added at the final concentration of 1×, and the sample was incubated at room temperature for 1 h. One hundred microliters of either soluble pollen proteins (5 mg mL^{-1}) or solubilized membrane proteins (3 mg mL^{-1}) was mixed with F-actin (350 μL at 0.36 mg mL^{-1}). When necessary, the final volume was adjusted to 500 μL with F-actin buffer (A buffer plus polymerization inducer in the ratio of 10:1 with the addition of 0.1% Triton X-100 in the case of membrane proteins). Controls were done by either assaying pollen proteins in the absence of F-actin or by replacing pollen proteins with BSA (20 μL at 3 mg mL^{-1}) or by analyzing the binding of pollen proteins to F-actin in the presence of 40 mM and 0.1 M Suc. Those concentrations of Suc were selected because Suc is reported to oscillate physiologically between 20 and 100 mM in plant cells (Gerhardt et al., 1987). Samples were incubated at room temperature for 30 to 60 min and then centrifuged at 150,000*g* for 60 min at 20°C over 0.5 mL of F-actin cushion buffer (5 mM Tris-HCl, pH 8.0, 2 mM $MgCl_2$, 50 mM KCl, and 10% glycerol).

The binding of cytoplasmic and membrane Sus to MTs was assayed by preparing a fraction of soluble and membrane pollen tube proteins as described above. Taxol-stabilized microtubules were prepared according to the method described by Cai et al. (2005). The affinity between Sus and MTs was evaluated by mixing 100 μL of either cytoplasmic or membrane pollen proteins with 200 μL of MT solution; the reaction volume was adjusted to 500 μL with taxol buffer. As controls, pollen proteins were analyzed without the addition of MTs; furthermore, pollen proteins were eventually replaced by BSA (20 μL at 3 mg mL^{-1}). In additional controls, Suc was also added at the final concentrations of 40 and 100 mM. Samples were incubated at room temperature for 30 min and then centrifuged at 100,000*g* for 40 min at 20°C over 0.5 mL of the MT cushion buffer (80 mM HEPES, pH 7.5, 1 mM EGTA, 1 mM $MgCl_2$, 10% Suc, and 20 μM taxol). Binding experiments were done at least three times, and blot assays were performed comparably.

Determination of Protein Concentration

The concentration of proteins was calculated with the method of Bradford (1976) using reagents supplied by Cytoskeleton. In the case of incompatible samples (such as those containing SDS), the 2-D Quant Kit (GE Healthcare) was used. Protocols were carried out according to the manufacturer's instructions using BSA as a standard. Each sample and standard were analyzed at least three times using a Shimadzu UV-160 spectrophotometer.

Image Analysis

Images of gels and chemiluminescence-developed immunoblots were captured with the Fluor-S Multi-Imager (Bio-Rad) using the software Quantity One (Bio-Rad). Gels and blots were subsequently analyzed using Quantity One software. The exposure time was 1 to 10 min for blots developed with chemiluminescence, 0.5 s for prestained molecular mass standards, and 5 to 7 s for gels stained with Coomassie Brilliant Blue. All images were processed correspondingly using the Autoscale command to improve the quality of gels/blots and the Background Subtraction command to remove the background noise (when present). The relative quantity of bands was eventually calculated with the Volume Tool of Quantity One software. To determine the molecular mass or immunoreactive bands, images of chemiluminescent signals were superimposed onto images of prestained molecular mass standards (Precision series; Bio-Rad) using the Multichannel Viewer of Quantity One.

Fluorescence intensity in microscope images was measured along the curvature of the pollen tube from the extreme tip down to the cell using ImageJ software (http://rsb.info.nih.gov/ij/; Calibrate and Plot Profile commands). Counting of fluorescent spots was done using the ImageJ software (Threshold and Analyze Particle commands) as described above for the counting of gold particles. In such cases, selected areas belong to the same focus plane. Measures are averages of 10 different pollen tubes at the same length. Graphics were made using Microsoft Excel. Quantitative valuation of colocalization between proteins was done using the JACoP plugin for ImageJ (http://rsb.info.nih.gov/ij/plugins/track/jacop.html). For quantitative analysis of immunoelectron microscope images, gold particles were counted in random selected images (about 30 images from different experiments) using ImageJ software with the command Analyze→Particle ("Threshold" option). In controls, the primary antibodies were omitted or the preimmune serum was used.

Sequence data from this article can be found in the GenBank/EMBL data libraries under accession numbers AF30437762.1 (NaGSL1) and AY337762.1 (AtGSL5).

Supplemental Data

The following materials are available in the online version of this article.

Supplemental Figure S1. Characterization of the anti-CalS DDA antibody.

Supplemental Figure S2. Relative quantitation profile of CesA, CalS, and Sus from three independent immunoblots performed on fractions of the Suc density gradient centrifugation.

Supplemental Figure S3. Time-course experiments of CalS distribution after treatment with inhibitors.

Supplemental Figure S4. Distribution of CalS after treatment with different inhibitors.

Supplemental Figure S5. Time-course experiments of CesA distribution after treatment with inhibitors.

Supplemental Figure S6. Fluorescence intensity of CesA measured along the pollen tube border.

Supplemental Figure S7. Staining of cellulose (left panel) and callose (right panel) with calcofluor white and aniline blue, respectively.

Supplemental Video S1. BDM-treated tube plus control.

Supplemental Video S2. BDM-treated tube.

ACKNOWLEDGMENTS

We thank Prof. Chris Somerville (Energy Biosciences Institute, University of California at Berkeley) for the generous gift of the anti-CesA antibody. We also thank Prof. Peter K. Hepler (Department of Biology, University of Massachusetts, Amherst) for critically reading and commenting on the manuscript. Finally, yet importantly, we gratefully acknowledge people working in the Botanical Garden of Siena University for assistance in plant growth.

Received December 18, 2010; accepted December 27, 2010; published December 29, 2010.

LITERATURE CITED

Aidemark M, Andersson CJ, Rasmusson AG, Widell S (2009) Regulation of callose synthase activity in situ in alamethicin-permeabilized Arabidopsis and tobacco suspension cells. BMC Plant Biol **9:** 27

Albrecht G, Mustroph A (2003) Localization of sucrose synthase in wheat roots: increased in situ activity of sucrose synthase correlates with cell wall thickening by cellulose deposition under hypoxia. Planta **217:** 252–260

Amor Y, Haigler CH, Johnson S, Wainscott M, Delmer DP (1995) A membrane-associated form of sucrose synthase and its potential role in synthesis of cellulose and callose in plants. Proc Natl Acad Sci USA **92:** 9353–9357

Anderson JR, Barnes WS, Bedinger P (2002) 2,6-Dichlorobenzonitrile, a

cellulose biosynthesis inhibitor, affects morphology and structural integrity of petunia and lily pollen tubes. J Plant Physiol **159:** 61–67

Aouar L, Chebli Y, Geitmann A (2010) Morphogenesis of complex plant cell shapes: the mechanical role of crystalline cellulose in growing pollen tubes. Sex Plant Reprod **23:** 15–27

Aström H (1992) Acetylated alpha-tubulin in the pollen tube microtubules. Cell Biol Int Rep **16:** 871–881

Astrom H, Sorri O, Raudaskoski M (1995) Role of microtubules in the movement of the vegetative nucleus and generative cell in tobacco pollen tubes. Sex Plant Reprod **8:** 61–69

Bove J, Vaillancourt B, Kroeger J, Hepler PK, Wiseman PW, Geitmann A (2008) Magnitude and direction of vesicle dynamics in growing pollen tubes using spatiotemporal image correlation spectroscopy and fluorescence recovery after photobleaching. Plant Physiol **147:** 1646–1658

Bradford MM (1976) A rapid and sensitive method for the quantitation of microgram quantities of protein utilizing the principle of protein-dye binding. Anal Biochem **72:** 248–254

Brownfield L, Ford K, Doblin MS, Newbigin E, Read S, Bacic A (2007) Proteomic and biochemical evidence links the callose synthase in Nicotiana alata pollen tubes to the product of the NaGSL1 gene. Plant J **52:** 147–156

Brownfield L, Wilson S, Newbigin E, Bacic A, Read S (2008) Molecular control of the glucan synthase-like protein NaGSL1 and callose synthesis during growth of Nicotiana alata pollen tubes. Biochem J **414:** 43–52

Buckeridge MS, Vergara CE, Carpita NC (1999) The mechanism of synthesis of a mixed-linkage (1→3), (1→4)β-D-glucan in maize: evidence for multiple sites of glucosyl transfer in the synthase complex. Plant Physiol **120:** 1105–1116

Cai G, Cresti M (2009) Organelle motility in the pollen tube: a tale of 20 years. J Exp Bot **60:** 495–508

Cai G, Cresti M (2010) Microtubule motors and pollen tube growth: still an open question. Protoplasma **247:** 131–143

Cai G, Ovidi E, Romagnoli S, Vantard M, Cresti M, Tiezzi A (2005) Identification and characterization of plasma membrane proteins that bind to microtubules in pollen tubes and generative cells of tobacco. Plant Cell Physiol **46:** 563–578

Cárdenas L, Lovy-Wheeler A, Kunkel JG, Hepler PK (2008) Pollen tube growth oscillations and intracellular calcium levels are reversibly modulated by actin polymerization. Plant Physiol **146:** 1611–1621

Cárdenas L, Lovy-Wheeler A, Wilsen KL, Hepler PK (2005) Actin polymerization promotes the reversal of streaming in the apex of pollen tubes. Cell Motil Cytoskeleton **61:** 112–127

Certal AC, Almeida RB, Carvalho LM, Wong E, Moreno N, Michard E, Carneiro J, Rodriguéz-Léon J, Wu HM, Cheung AY, et al (2008) Exclusion of a proton ATPase from the apical membrane is associated with cell polarity and tip growth in *Nicotiana tabacum* pollen tubes. Plant Cell **20:** 614–634

Chaffey N, Barlow P (2002) Myosin, microtubules, and microfilaments: cooperation between cytoskeletal components during cambial cell division and secondary vascular differentiation in trees. Planta **214:** 526–536

Chen XY, Kim JY (2009) Callose synthesis in higher plants. Plant Signal Behav **4:** 489–492

Cheung AY (1996) Pollen-pistil interactions during pollen-tube growth. Trends Plant Sci **1:** 45–51

Cheung AY, Duan QH, Costa SS, de Graaf BH, Di Stilio VS, Feijo J, Wu HM (2008) The dynamic pollen tube cytoskeleton: live cell studies using actin-binding and microtubule-binding reporter proteins. Mol Plant **1:** 686–702

Chourey PS, Taliercio EW, Carlson SJ, Ruan YL (1998) Genetic evidence that the two isozymes of sucrose synthase present in developing maize endosperm are critical, one for cell wall integrity and the other for starch biosynthesis. Mol Gen Genet **259:** 88–96

Cole RA, Fowler JE (2006) Polarized growth: maintaining focus on the tip. Curr Opin Plant Biol **9:** 579–588

Cresti M, van Went JL (1976) Callose deposition and plug formation in *Petunia* pollen tubes in situ. Planta **133:** 35–40

Crowell EF, Bischoff V, Desprez T, Rolland A, Stierhof YD, Schumacher K, Gonneau M, Höfte H, Vernhettes S (2009) Pausing of Golgi bodies on microtubules regulates secretion of cellulose synthase complexes in *Arabidopsis*. Plant Cell **21:** 1141–1154

DeBolt S, Gutierrez R, Ehrhardt DW, Melo CV, Ross L, Cutler SR, Somerville C, Bonetta D (2007a) Morlin, an inhibitor of cortical microtubule dynamics and cellulose synthase movement. Proc Natl Acad Sci USA **104:** 5854–5859

DeBolt S, Gutierrez R, Ehrhardt DW, Somerville C (2007b) Nonmotile cellulose synthase subunits repeatedly accumulate within localized regions at the plasma membrane in Arabidopsis hypocotyl cells following 2,6-dichlorobenzonitrile treatment. Plant Physiol **145:** 334–338

de Graaf BHJ, Cheung AY, Andreyeva T, Levasseur K, Kieliszewski M, Wu HM (2005) Rab11 GTPase-regulated membrane trafficking is crucial for tip-focused pollen tube growth in tobacco. Plant Cell **17:** 2564–2579

Del Casino C, Li Y, Moscatelli A, Scali M, Tiezzi A, Cresti M (1993) Distribution of microtubules during the growth of tobacco pollen tubes. Biol Cell **79:** 125–132

Desprez T, Juraniec M, Crowell EF, Jouy H, Pochylova Z, Parcy F, Höfte H, Gonneau M, Vernhettes S (2007) Organization of cellulose synthase complexes involved in primary cell wall synthesis in Arabidopsis thaliana. Proc Natl Acad Sci USA **104:** 15572–15577

Duncan KA, Huber SC (2007) Sucrose synthase oligomerization and F-actin association are regulated by sucrose concentration and phosphorylation. Plant Cell Physiol **48:** 1612–1623

Ferguson C, Teeri TT, Siika-aho M, Read SM, Bacic A (1998) Location of cellulose and callose in pollen tubes and grains of *Nicotiana tabacum*. Planta **206:** 452–460

Fujii S, Hayashi T, Mizuno K (2010) Sucrose synthase is an integral component of the cellulose synthesis machinery. Plant Cell Physiol **51:** 294–301

Geitmann A, Emons AM (2000) The cytoskeleton in plant and fungal cell tip growth. J Microsc **198:** 218–245

Gerhardt R, Stitt M, Heldt HW (1987) Subcellular metabolite levels in spinach leaves: regulation of sucrose synthesis during diurnal alterations in photosynthetic partitioning. Plant Physiol **83:** 399–407

Gillmor CS, Poindexter P, Lorieau J, Palcic MM, Somerville C (2002) α-Glucosidase I is required for cellulose biosynthesis and morphogenesis in Arabidopsis. J Cell Biol **156:** 1003–1013

Gossot O, Geitmann A (2007) Pollen tube growth: coping with mechanical obstacles involves the cytoskeleton. Planta **226:** 405–416

Goubet F, Misrahi A, Park SK, Zhang Z, Twell D, Dupree P (2003) AtCSLA7, a cellulose synthase-like putative glycosyltransferase, is important for pollen tube growth and embryogenesis in Arabidopsis. Plant Physiol **131:** 547–557

Guerriero G, Fugelstad J, Bulone V (2010) What do we really know about cellulose biosynthesis in higher plants? J Integr Plant Biol **52:** 161–175

Gutierrez R, Lindeboom JJ, Paredez AR, Emons AM, Ehrhardt DW (2009) Arabidopsis cortical microtubules position cellulose synthase delivery to the plasma membrane and interact with cellulose synthase trafficking compartments. Nat Cell Biol **11:** 797–806

Hardin SC, Winter H, Huber SC (2004) Phosphorylation of the amino terminus of maize sucrose synthase in relation to membrane association and enzyme activity. Plant Physiol **134:** 1427–1438

Heinlein M, Starlinger P (1989) Tissue- and cell-specific expression of the two sucrose synthase isoenzymes in developing maize kernels. Mol Gen Genet **215:** 441–446

Higashiyama T, Kuroiwa H, Kuroiwa T (2003) Pollen-tube guidance: beacons from the female gametophyte. Curr Opin Plant Biol **6:** 36–41

Hong Z, Zhang Z, Olson JM, Verma DP (2001) A novel UDP-glucose transferase is part of the callose synthase complex and interacts with phragmoplastin at the forming cell plate. Plant Cell **13:** 769–779

Ian B, Jonathan T, Maria K, John M, Paul B (1998) Localization of components of the oxidative cross-linking of glycoproteins and of callose synthesis in papillae formed during the interaction between non-pathogenic strains of *Xanthomonas campestris* and French bean mesophyll cells. Plant J **15:** 333–343

Ketelaar T, de Ruijter NCA, Emons AM (2003) Unstable F-actin specifies the area and microtubule direction of cell expansion in *Arabidopsis* root hairs. Plant Cell **15:** 285–292

Ketelaar T, Galway ME, Mulder BM, Emons AMC (2008) Rates of exocytosis and endocytosis in *Arabidopsis* root hairs and pollen tubes. J Microsc **231:** 265–273

Kimura S, Laosinchai W, Itoh T, Cui X, Linder CR, Brown RM Jr (1999) Immunogold labeling of rosette terminal cellulose-synthesizing complexes in the vascular plant *Vigna angularis*. Plant Cell **11:** 2075–2086

Konishi T, Ohmiya Y, Hayashi T (2004) Evidence that sucrose loaded into the phloem of a poplar leaf is used directly by sucrose synthase

associated with various β-glucan synthases in the stem. Plant Physiol **134:** 1146–1152

Kroh M, Knuiman B (1982) Ultrastructure of cell wall and plugs of tobacco pollen tubes after chemical extraction of polysaccharides. Planta **154:** 241–250

Kroh M, Knuiman B (1985) Exocytosis in non-plasmolyzed and plasmolyzed tobacco pollen tubes. Planta **166:** 287–299

Laitiainen E, Nieminen KM, Vihinen H, Raudaskoski M (2002) Movement of generative cell and vegetative nucleus in tobacco pollen tubes is dependent on microtubule cytoskeleton but independent of the synthesis of callose plugs. Sex Plant Reprod **15:** 195–204

Lenartowska M, Michalska A (2008) Actin filament organization and polarity in pollen tubes revealed by myosin II subfragment 1 decoration. Planta **228:** 891–896

Li YQ, Croes AF, Linskens HF (1983) Cell-wall proteins in pollen and roots of *Lilium longiflorum*: extraction and partial characterization. Planta **158:** 422–427

Li YQ, Faleri C, Geitmann A, Zhang HQ, Cresti M (1995) Immunogold localization of arabinogalactan proteins, unesterified and esterified pectins in pollen grains and pollen tubes of *Nicotiana tabacum* L. Protoplasma **189:** 26–36

Lloyd C, Chan J (2008) The parallel lives of microtubules and cellulose microfibrils. Curr Opin Plant Biol **11:** 641–646

Lovy-Wheeler A, Wilsen KL, Baskin TI, Hepler PK (2005) Enhanced fixation reveals the apical cortical fringe of actin filaments as a consistent feature of the pollen tube. Planta **221:** 95–104

Lucas J, Shaw SL (2008) Cortical microtubule arrays in the Arabidopsis seedling. Curr Opin Plant Biol **11:** 94–98

Matic S, Akerlund HE, Everitt E, Widell S (2004) Sucrose synthase isoforms in cultured tobacco cells. Plant Physiol Biochem **42:** 299–306

Miller DD, de Ruijter NCA, Bisseling T, Emons AMC (1999) The role of actin in root hair morphogenesis: studies with lipochito-oligosaccharide as a growth stimulator and cytochalasin as an actin perturbing drug. Plant J **17:** 141–154

Miller DD, Ruijter NCA, Emons AM (1997) From signal to form: aspects of the cytoskeleton-plasma membrane-cell wall continuum in root hair tips. J Exp Bot **48:** 1881–1896

Mutwil M, Debolt S, Persson S (2008) Cellulose synthesis: a complex complex. Curr Opin Plant Biol **11:** 252–257

Nebenführ A, Ritzenthaler C, Robinson DG (2002) Brefeldin A: deciphering an enigmatic inhibitor of secretion. Plant Physiol **130:** 1102–1108

Olmsted JB (1981) Affinity purification of antibodies from diazotized paper blots of heterogeneous protein samples. J Biol Chem **256:** 11955–11957

Østergaard L, Petersen M, Mattsson O, Mundy J (2002) An Arabidopsis callose synthase. Plant Mol Biol **49:** 559–566

Paredez AR, Somerville CR, Ehrhardt DW (2006) Visualization of cellulose synthase demonstrates functional association with microtubules. Science **312:** 1491–1495

Parrotta L, Cai G, Cresti M (2010) Changes in the accumulation of α- and β-tubulin during bud development in *Vitis vinifera* L. Planta **231:** 277–291

Parton RM, Fischer-Parton S, Trewavas AJ, Watahiki MK (2003) Pollen tubes exhibit regular periodic membrane trafficking events in the absence of apical extension. J Cell Sci **116:** 2707–2719

Parton RM, Fischer-Parton S, Watahiki MK, Trewavas AJ (2001) Dynamics of the apical vesicle accumulation and the rate of growth are related in individual pollen tubes. J Cell Sci **114:** 2685–2695

Pear JR, Kawagoe Y, Schreckengost WE, Delmer DP, Stalker DM (1996) Higher plants contain homologs of the bacterial celA genes encoding the catalytic subunit of cellulose synthase. Proc Natl Acad Sci USA **93:** 12637–12642

Persia D, Cai G, Del Casino C, Faleri C, Willemse MTM, Cresti M (2008) Sucrose synthase is associated with the cell wall of tobacco pollen tubes. Plant Physiol **147:** 1603–1618

Persson S, Paredez A, Carroll A, Palsdottir H, Doblin M, Poindexter P, Khitrov N, Auer M, Somerville CR (2007) Genetic evidence for three unique components in primary cell-wall cellulose synthase complexes in Arabidopsis. Proc Natl Acad Sci USA **104:** 15566–15571

Reiss HD, Herth W, Schnepf E (1985) Plasma-membrane "rosettes" are present in the lily pollen tube. Naturwissenschaften **72:** 276

Richmond TA, Somerville CR (2000) The cellulose synthase superfamily. Plant Physiol **124:** 495–498

Robinson DG, Hinz G (2001) Organelle isolation. *In* C Hawes, B Satiat-Jeunemaitre, eds, Plant Cell Biology, Ed 2. Oxford University Press, Oxford, pp 295–323

Rutten TL, Knuiman B (1993) Brefeldin A effects on tobacco pollen tubes. Eur J Cell Biol **61:** 247–255

Salnikov VV, Grimson MJ, Delmer DP, Haigler CH (2001) Sucrose synthase localizes to cellulose synthesis sites in tracheary elements. Phytochemistry **57:** 823–833

Salnikov VV, Grimson MJ, Seagull RW, Haigler CH (2003) Localization of sucrose synthase and callose in freeze-substituted secondary-wall-stage cotton fibers. Protoplasma **221:** 175–184

Samaj J, Peters M, Volkmann D, Baluska F (2000) Effects of myosin ATPase inhibitor 2,3-butanedione 2-monoxime on distributions of myosins, F-actin, microtubules, and cortical endoplasmic reticulum in maize root apices. Plant Cell Physiol **41:** 571–582

Scherp P, Grotha R, Kutschera U (2002) Interaction between cytokinesis-related callose and cortical microtubules in dividing cells of the liverwort *Riella helicophylla*. Plant Biol **4:** 619–624

Schlupmann H, Bacic A, Read SM (1994) Uridine diphosphate glucose metabolism and callose synthesis in cultured pollen tubes of *Nicotiana alata* Link et Otto. Plant Physiol **105:** 659–670

Tominaga M, Yokota E, Sonobe S, Shimmen T (2000) Mechanism of inhibition of cytoplasmic streaming by a myosin inhibitor, 2,3-butanedione monoxime. Protoplasma **213:** 46–54

Turner A, Bacic A, Harris PJ, Read SM (1998) Membrane fractionation and enrichment of callose synthase from pollen tubes of *Nicotiana alata* Link et Otto. Planta **205:** 380–388

Verma DP, Hong Z (2001) Plant callose synthase complexes. Plant Mol Biol **47:** 693–701

Vidali L, Hepler PK (2001) Actin and pollen tube growth. Protoplasma **215:** 64–76

Vidali L, McKenna ST, Hepler PK (2001) Actin polymerization is essential for pollen tube growth. Mol Biol Cell **12:** 2534–2545

Wang W, Vignani R, Scali M, Cresti M (2006) A universal and rapid protocol for protein extraction from recalcitrant plant tissues for proteomic analysis. Electrophoresis **27:** 2782–2786

Wightman R, Turner S (2010) Trafficking of the plant cellulose synthase complex. Plant Physiol **153:** 427–432

Wightman R, Turner SR (2008) The roles of the cytoskeleton during cellulose deposition at the secondary cell wall. Plant J **54:** 794–805

Winter H, Huber JL, Huber SC (1998) Identification of sucrose synthase as an actin-binding protein. FEBS Lett **430:** 205–208

Yasuhara H (2005) Caffeine inhibits callose deposition in the cell plate and the depolymerization of microtubules in the central region of the phragmoplast. Plant Cell Physiol **46:** 1083–1092

Zhang Y, He J, Lee D, McCormick S (2010) Interdependence of endomembrane trafficking and actin dynamics during polarized growth of Arabidopsis pollen tubes. Plant Physiol **152:** 2200–2210